Final Report

OIL-BATH AIR CLEANERS

Operating Principles and Performance Characteristics

Seymour Calvert
J. Louis York

engl
UHR1088

engl
UHR1088

TABLE OF CONTENTS

CHAPTER I

OBJECTIVES AND SUMMARY

This report is the final summary of the research program performed for the Detroit Arsenal under Contract No. DA-20-089-ORD-36962 (Engineering Research Institute Project No. 2233). The program consisted of two parts. One was an investigation of snow and ice accumulation in air induction systems and the other was a study of the performance of induction air cleaners and their principles of operation.

Progress on this program was reported to Mr. C. R. Denton of the Engine Branch, Research and Development, Detroit Arsenal. These included both oral and written reports which were transmitted as the progress had reached definite stages. Substantial progress was made on both parts of the program, but work was slowed for the last half of the period and eventually halted for lack of funds. Long strides can be made in this area, based on the knowledge gained.

The areas of interest in the program were defined in the contracts and are restated here, followed by a summary of the action.

ICE AND SNOW INVESTIGATION

"OBJECTIVE:

"To perform an engineering investigation and study into methods of safeguarding military vehicles against snow and ice accumulation in the air induction system.

"REQUIREMENTS:

"A. The Contractor...shall furnish...a study of the effects of snow and ice accumulation in air induction systems of military vehicles which shall include, but not be limited to the following:

1. A study of the causes of snow clouds and their characteristics.

2. A study of characteristics of vehicles which influence the formation of snow clouds.

3. A study of Meteorological conditions such as temperature, winds, ice and snow crystalline structure which are conducive to cloud formation.

4. Analysis of the flow of air through the induction systems of the vehicles encountering the accumulation of ice and snow.

5. Effects of the geometrical arrangements of the air induction system.

6. Effects of components such as filters and carburetors.

7. Effects of the nature and type of snow and ice crystals suspended in air.

"B. Upon conclusion of the studies...above, the Contractor shall perform an engineering investigation and evaluation of methods leading to an elimination of ice and snow accumulation in the air induction system."

This investigation was divided into two parts. A study of the general properties of snow and ice was made and their influence on air induction systems and air cleaners in particular was examined. The results are presented in Interim Technical Report No. 5, "Effectiveness of Air Cleaners Operating in Atmospheres Containing Snow," by R. J. Dean, A. Weir, C. Iott, S. H. Reich, and R. B. Morrison, November, 1956.

An experimental study on a quarter-section Donaldson oil-bath air cleaner showed that part of the induced snow will remain in either a wet or dry air-cleaner reservoir, part will be trapped in the filter element, and part will pass downstream into the air induction system. Snow collection efficiency in the air cleaner is a function principally of reservoir fluid temperature and the rate of snow induction. Collection efficiencies are generally less than 80 percent. Air-cleaner pressure losses reach a maximum and air flow rate a minimum for a given snow volume in the cleaner. Addition of more snow does not change these values for this "blocked" condition. Snow in the air cleaner may reduce the air flow rate by a factor of nearly four.

A supplement to the report on this program is a time-lapse motion picture showing an air-cleaner section in operation on air containing snow.

This program indicates that a precleaner might improve the overall performance of the snow-removal system, especially if adequate continuous removal of collected snow from the precleaner can be worked out.

AIR CLEANER INVESTIGATION

"OBJECTIVE:

"To perform an engineering investigation study into the performance of induction air cleaners and their principles of operation.

"REQUIREMENTS:

"The Contractor...shall,...accomplish the following:

1. Conduct a study into the performance of air cleaners and their principles of operation, [with] the objectives of:

a. Determining the basic principles involved in the mechanism of operation of existing air cleaners and measuring the limits and quantitative effect of these principles on performance, with first emphasis upon the oil bath units now employed extensively.

b. Organizing these principles and quantitative measurements to furnish a basis for evaluating new design, developing improvements in existing cleaners, and developing new designs.

c. Furnishing technical background for preparation of revised specifications for air cleaners.

2. The above study shall be conducted in accordance with, but shall not be limited to, the following procedure:

a. The Contractor shall gather existing information on principles and performance of various air cleaners by thorough review of the technical literature, interviews with personnel of the armed services, examination of service reports on performance and maintenance, and interviews with manufacturers of air cleaners.

b. The Contractor shall conduct experimental studies on cleaners to determine flow patterns, comparative performance of individual components of different design and construction material, and effect of varying operating conditions. These will include photographic studies of performance, measurement of pressure losses, dust removal and oil losses.

c. The Contractor shall prepare modified and experimental cleaners and instrumentation for the study of cleaners, and cooperate in testing of such cleaners, under standard conditions, in Government laboratories, for comparison with routine Government tests.

d. The Contractor shall analyze and interpret the results of parts (a) and (c) and prepare interim technical reports and evaluations of cleaners, procedures and designs as progress warrants, including the furnishing of the technical background and assistance necessary for the preparation of specifications."

The following written reports were submitted:

1. Interim Technical Report No. 1, "The Prediction of Dust Removal in an Oil-Bath Air Cleaner," by Seymour Calvert, July, 1954.

2. Interim Technical Report No. 2, "Evaluation of Proposed Test Methods for Air Cleaners," by Seymour Calvert, J. L. York, Thomas E. Slykhouse, and Donald M. Arveson, March, 1955.

3. Interim Technical Report No. 3, "The Performance of Packed Sections in Oil-Bath Air Cleaners," by Seymour Calvert, May, 1955.

4. Interim Technical Report No. 4, "Pressure Drop and Flow Patterns in the Impingement Section of an Oil-Bath Air Cleaner," by Seymour Calvert, Henry J. Hartog, Hadley J. Smith, Robert M. Pease, and J. Louis York, May, 1955.

5. Interim Technical Report No. 6, "The Collection of Salt Dust on Dry Wires," by Seymour Calvert, (presented as Appendix C of this summary report).

This investigation dealt primarily with oil-bath air cleaners although some of the results are applicable to other types of air cleaners. In the oil-bath air cleaner there are two major zones of action. The first zone encountered by the air is the impingement section in which the air stream is deflected by a relatively large conduit element and simultaneously is contacted with oil. The second zone is the packed section in which the air stream leaving the impingement section passes through an array of small solid bodies such as wire screen or other fibrous packing. The functions of the impingement section are to remove larger dust particles and to'introduce oil which is carried to the packed section. The functions of the packed section are to remove the smaller dust particles and also to separate the entrained oil from the air stream.

The research work was aimed at attaining an understanding of these functions and at developing design methods which would enable the prediction of the characteristics of the basic air-cleaner elements. This involved the following steps:

A. Concerning the Performance of the Impingement Section

    1. Methods for predicting the dust collection efficiency from theoretical considerations were applied and appeared to be adequate. Because the dust collection efficiency of the impingement section is considerably lower than that of the packed section, it is not a critical component of overall collection efficiency.

    2. The effect of geometry on the relationship between air flow rate and pressure drop was evaluated both experimentally and theoretically. Design methods were developed for the prediction of this relationship. Oil flow was found to have a negligible effect on this relationship at higher air flow rates.

    3. Flow patterns were studied by means of both smoke streams in an air-flow model and tracer particles in a water-flow model. The characteristics of the flow patterns and the effects of geometric changes are presented in photographs and drawings.

B. Concerning the Performance of the Packed Section

    1. A method for predicting dust collection efficiency from theoretical considerations was compared with experimental data. The prediction seems adequate for wetted packing but is considerably in error for dry packing (wires).

    2. A method for predicting the relationship between air flow rate and pressure drop has been developed and is adequate for design purposes. The effect of oil flow on this relationship is negligible below the flooding point.

    3. Flooding points have been correlated as functions of fluid flow rates, fluid properties, and packing properties.

C. Concerning Test Methods for the Determination of Dust Collection Efficiency

    1. The two methods used in this work involved the use of solid particles as the test dust. Dispersed silica dust and spray-dried salt dust were employed.

    2. Several alternate test methods were evaluated for possible use in future work. A technique based on analysis by means of light-scattering measurements appears to be the most promising.

CHAPTER II

DISCUSSION OF RESULTS

The results of this investigation have been set forth previously in Interim Technical Reports, with the exception of the material covered in Reports 5 and 6, appearing simultaneously with this report. In all cases a complete exposition of the work is given in the interim reports and we shall not include all of the details here. Rather, it is our intent to summarize and integrate the major findings and to guide the reader to the interim reports for further detail. We will first discuss the impingement section, next the packed section, and, finally, test methods.

THE IMPINGEMENT SECTION

The physical nature of the impingement section is shown in Figs. 18 and 25 from Interim Technical Report No. 4 (see Appendix A, page 54, and Appendix B, page 68), which show a detailed sketch of the impingement section of the cleaner and a half-section through a Donaldson air cleaner. This particular air cleaner is representative of the best designs available commercially. In operation at normal or high speed, most of the oil which originally filled the baffle cup is blown out of the cup. Most of the oil contacting the air under this condition enters the air stream either by overflowing the edge of the cup or by flowing down the periphery of the central tube.

The two major questions concerning the impingement section are how to predict its dust collection efficiency and how to predict its pressure-loss characteristics. Prediction of dust collection efficiency was covered in Interim Technical Report No. 1.

Two methods of prediction, both based on a description of particle trajectories as influenced by particle inertia and drag exerted by the air stream, were employed. The first method was derived from the premise that the trajectory of a particle in a turning air stream may be approximated as that which it would follow if the air made an angular rather than a curved turn. The particle was assumed to be thrown into still air at a given initial velocity and the distance it would travel before being stopped by the air

resistance was calculated. If this distance is at least equal to the particle's distance from the baffle cup, the particle will strike the baffle.

The second method was based on the Ranz and Wong data[2] for the collection efficiency of round and rectangular jets striking flat plates. It was assumed that the impingement section could be considered to be a round jet followed by a rectangular jet. The dimensions of the rectangular jet are given by the width of the air stream at the vena contracta after the first bend (round jet) and the circumference of the circle passing through the same position.

The two methods gave practically identical results. The predicted collection efficiency of the impingement section in a Donaldson cleaner running at full capacity was about 48 percent for AC fine dust and 79 percent for AC coarse dust. The impingement section has the characteristic of removing substantially all dust larger than about 15-micron diameter and substantially none smaller than 5-micron diameter.

Because the use of the Ranz and Wong data is much simpler than the other method, it is recommended. Briefly, this method is based on the use of a graphical relationship between collection efficiency and a collection parameter, ψ. The relationship is valid where the motion of the particles may be described by Stokes' Law. It is shown in Fig. 1 (Fig. 6 from I.T.R. 1).

The terms in the parameter, ψ, are as follows:

C = a dimensionless correction for slip flow which is substantially equal to 1 for particles larger than 1 micron,

ρ_p = particle density,

V_o = average velocity of gas stream,

μ = gas viscosity, and

D_c = jet width or diameter.

The pressure drop and flow patterns for the impingement section were covered in Interim Technical Report No. 4. As described in that report, the results were as follows:

"Our main interest in the impingement section centers around its effect on the flow of air. It functions incidentally to provide a flow of oil into the packed section and to establish a tranquil zone in which collected dust can settle out of the oil. The two main questions whose study is reported here are:
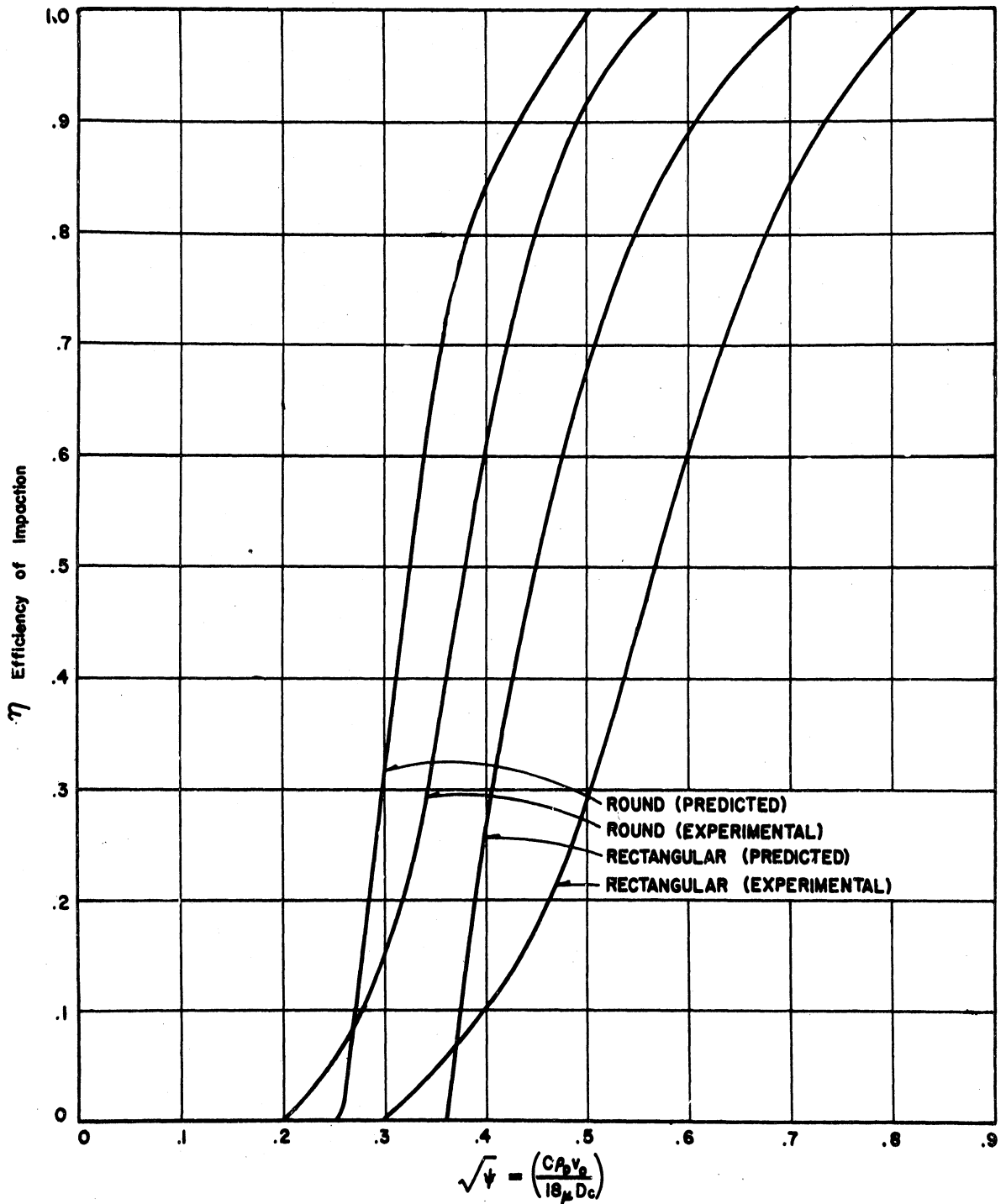
Fig. 1. Predicted and experimental impaction efficiencies for Aerosol jets from: Ranz and Wong I and EC 44, 1371.

1. What is the relationship between pressure drop, air flow rate, impingement section geometry, and oil flow rate?

2. What are the flow patterns in the impingement section and in the air stream just entering the packed section?

"Chapters I and II [of I.T.R. 4] deal with the first question. Experimental work on the flow of air through various models of impingement section geometry is described in Chapter I. Analyses of the data gave an empirical relationship between pressure drop, air flow rate, and geometric parameters such as tube and baffle sizes and the distance between the tube outlet and the baffle.

"This relationship is valid over a wide range of geometric parameters and provides a convenient method for prediction of pressure drop for air flow through baffled systems such as the impingement section. The data on two-phase flow (air and oil) showed that at high flow rates the behavior of the two-phase system can be described by the single-phase relationships with accuracy which is adequate for design purposes.

"An analysis of the problem of air flow through baffled systems of this type is given in Chapter II. The result of the analysis is a generalized method, based on ideal fluid-flow theory, which predicts pressure drop versus flow rate relationships which agree satisfactorily with both the data on experimental impingement-section models and the data on a production-model Donaldson Company air cleaner. Experimental data on the pressure drop versus flow relationship for a production-model Donaldson Company 410 cfm air cleaner are also presented and analyzed in this chapter. Possible design modifications are indicated which would alleviate the undesirable conditions of high pressure drop in the entry section and uneven flow distribution in the outlet section of this cleaner.

"Flow visualization experiments on impingement section models are described in Chapter III. The principal methods of determining the flow patterns involved visual observation and were a smoke-stream technique used on a three-dimensional model and a free-surface water-tunnel technique used on a two-dimensional model. Photographs and drawings of these experiments show the flow patterns encountered. Design modifications are suggested for attaining more desirable flow characteristics. The velocity distribution in the stream entering the packed section is uniform in almost all (geometric) cases."

The correlation derived from experimental data consists of an equation with one empirical constant and a graphical relationship between the constant and geometric parameters. The equation is:

$$\Delta P = K\rho \frac{V^2}{2g} \, . \qquad (1)$$

The variables involved are:

ΔP = pressure drop for the turn (lb/ft^2),

V = average velocity in the center tube (air inlet to baffle) (ft/sec),

ρ = air density (lb/ft^3),

h = baffle spacing (distance from end of center tube to baffle) (inches),

D = baffle diameter (inches),

H = baffle rim height (inches),

d = center tube diameter (inches), and

g = 32.2 ft/sec^2.

The relationship between K and the geometric variables is shown in Fig. 2 (Fig. 9 from I.T.R. 4).

A more rigorous and general relationship was derived in Chapter II of Interim Technical Report No. 4. Because of its complexity, it is not advisable to take the equations out of context and since this is a very important part of the design method it appears desirable to reproduce this chapter photographically as Appendix A.

The discussion of flow patterns cannot be condensed intelligibly, therefore Chapter III of Interim Technical Report No. 4 is also reproduced photographically as Appendix B.

THE PACKED SECTION

The physical nature of the packed section is illustrated in Fig. 25 of Interim Technical Report No. 4 (Appendix B, page 68), where it includes the first screen and the distributed screen. In operation the air leaving the baffle cup carries oil along with it into the packing. The entrained oil is separated from the air by collision with the packing elements and returns to the impingement section by running down the outer wall and the outside of the center tube.

The major functions of the packed section are to collect dust which has escaped the impingement zone and to prevent the carry-over of oil. The oil, which is blown into the packing from the impingement section, washes the packing fibers clean and acts as an adhesive for the retention of dust.
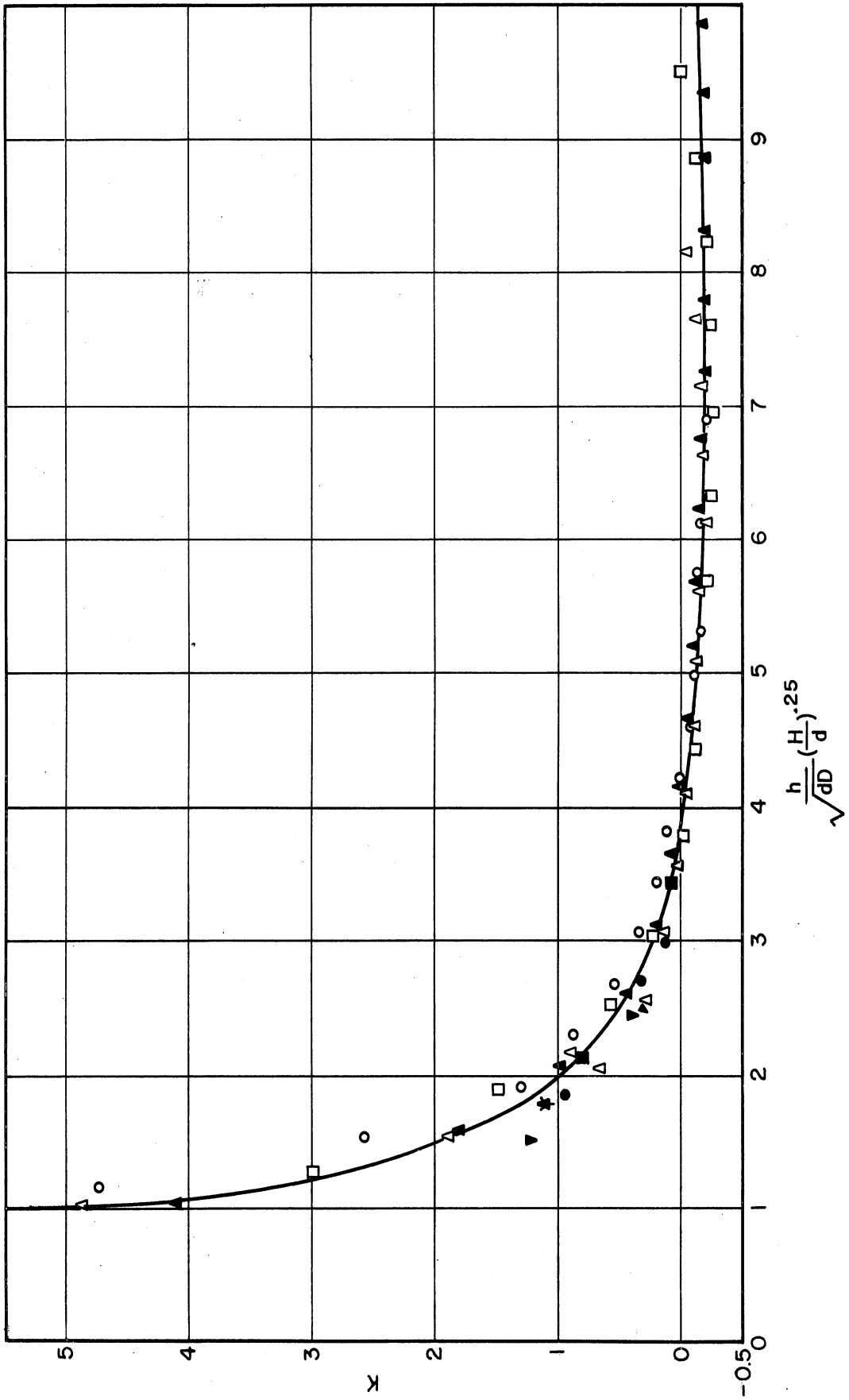
Fig. 2. Air-cleaner tests. K in terms of cleaner geometry.

The major point of interest concerns the mechanism by which fibrous elements collect dust and the possibility of predicting collection efficiency. In I.T.R. 1 it was proposed that collection by impingement seemed the most likely mechanism and presented a method for computing the collection efficiency for fibers. Following that, there remained the task of obtaining experimental verification of the theoretical analysis. Consequently, an experimental investigation of dust collection efficiency was initiated. Several months after this, a paper concerning an investigation of the collection efficiency of metal wool fibers was presented; and the data established the validity of the theoretical method of prediction. As a result of this good fortune, it was not necessary to continue with as extensive a program as originally planned, although it seemed advisable to get some limited data on the collection efficiency of round wires and to evaluate the effect of mixing in the air stream within the bed.

Another significant point of interest concerns the functions of fibrous packing as an oil entrainment separator. It very quickly becomes apparent that the problem here is not one of capturing the oil drops, since this is easily done, but rather of preventing the re-entrainment of drops due to the flooding of the packing. This phenomenon is seen as "oil carry-over" in air-cleaner operation and it is this which dictates the upper limit of air-cleaner capacity. Consequently, the determination of flooding points was included in the experimental program. Also included in the experimental program was the study of pressure drop for air flow through fiber beds.

The experimental data on the behavior of packing materials have been obtained from the operation of packed columns which did not include an impingement section.

The dust collection efficiency was predicted and determined experimentally. Efficiency can be predicted quite well for wetted wires, but it cannot be for dry wires. The subject is covered in Interim Technical Reports Nos. 1, 3, and 6. A brief introduction to the subject is given in Report No. 3.

A preliminary study of the literature on the subject of aerosol collection resulted in the belief that the principal mechanism of collection in an oil-bath air cleaner is by impaction. In other words, the principal force causing the separation of a dust particle from the air stream is inertia. The behavior of particles subjected to inertial forces when an air stream passes around solid objects has been studied by several investigators and the equations describing the particle trajectories have been solved. These data on particle trajectories have been interpreted in terms of collection efficiency and this interpretation is presented in graphical form.[2]

A plot of collection efficiency versus the collection parameter is shown in Fig. 3 (Fig. 1 from I.T.R. 3). This plot shows the fraction of the particles originally traveling toward the target which will strike it. It
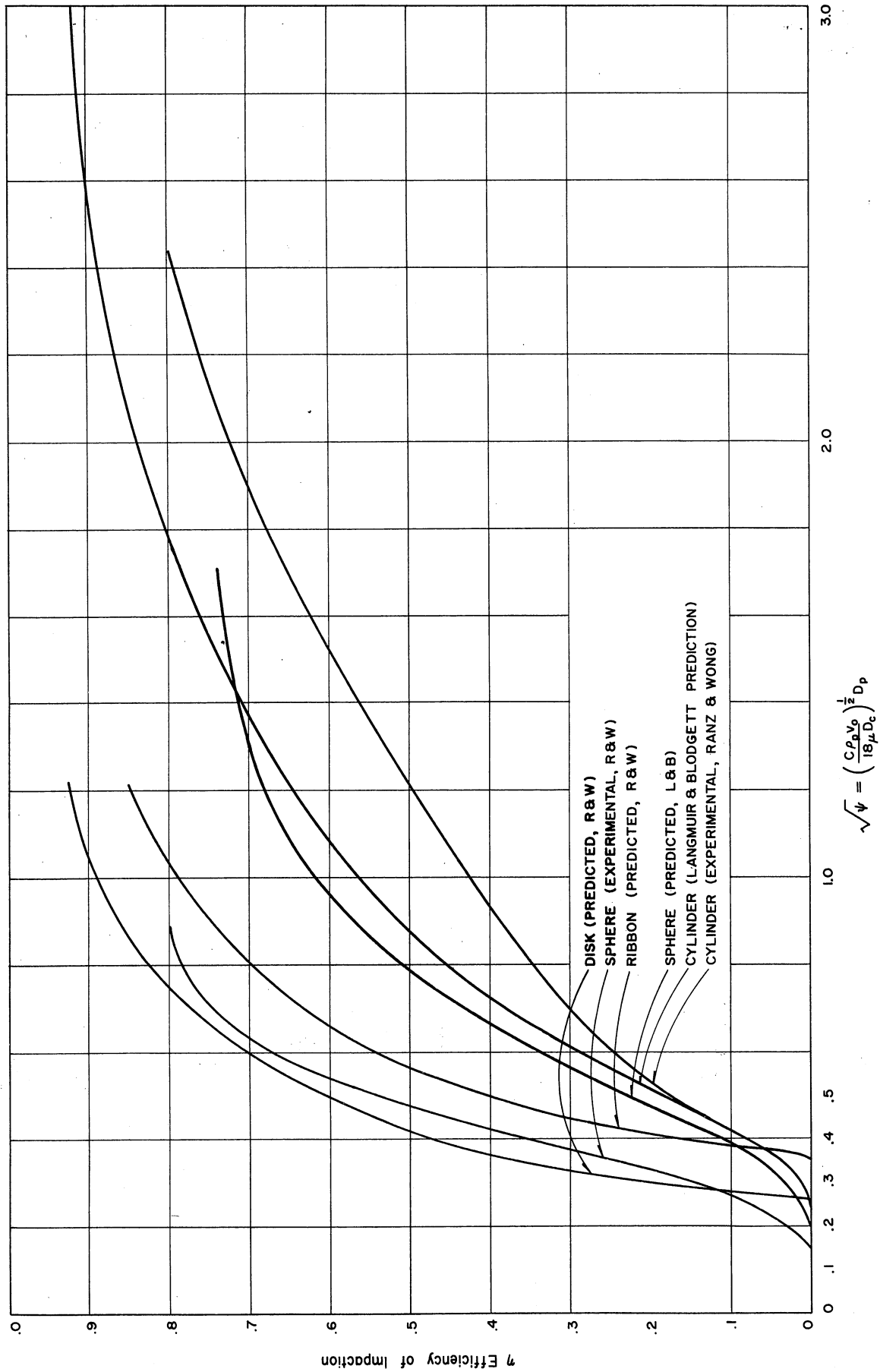
Fig. 3. Predicted and experimental impaction efficiencies for collectors of various shapes.[2]

can be seen that the collection efficiency depends on the particle size and density, the gas velocity and viscosity, and the collection diameter. Efficiency increases with increasing particle size and gas velocity, and decreases with increasing collector size.

One method by which this information may be applied to the prediction of packed-section collection efficiency has been fully described in Interim Technical Report No. 1. An illustrative example was given for a section of screen packing similar to the lower element in a production-model of a Donaldson oil-bath air cleaner such as is presently used on tank engines. The efficiency prediction has been worked out in more detail since then and the results are given in Table I.

TABLE I

PREDICTED COLLECTION EFFICIENCY FOR THE PACKED
SECTION OF A DONALDSON COMPANY
NO. A-14111 OIL-BATH AIR CLEANER

Stage	Component	Air Velocity, ft/sec	Fine Dust Collection Efficiency of Air Cleaner, %
1	Removable element, 7 layers of 14-mesh screen, 0.0165" wire diameter.	50 25* 16.7 12.5	86.9 80.4 76.5 74.2
2	First fixed element, 12 layers of crimped 8-mesh hardware cloth, 0.015" wire diameter.	12.5*	88.7**
3	Final fixed element, 26 turns of crimped 12-mesh screen, 3" deep, 0.0105" wire diameter.	12.5*	90.66**

*Velocity at rated capacity.
**Cumulative efficiency, including that of previous stage(s) at rated capacity.

The data in Table I show the effect of air velocity on collection efficiency in the first stage, as well as the decreasing contribution to efficiency made by the following stages. It is interesting to note that while an increase in velocity from 25 to 50 feet per second in Stage 1 gives almost as great an increase in efficiency as does the addition of Stage 2 at rated

velocities, it is not accomplished in the same way. The increase in velocity results in a higher collection efficiency for small particles, while the increase in bed depth, even though at a lower velocity, results in a greater total collection efficiency for particles larger than the minimum size. This is indicated by the predicted efficiencies for various particle sizes, as given in Table II.

TABLE II

PREDICTED COLLECTION EFFICIENCY FOR VARIOUS
PARTICLE SIZES IN EACH OF THE PACKED STAGES
OF A DONALDSON COMPANY NO. A-14111 OIL-BATH CLEANER

Particle Dia, micron	Collection Efficiency, %			
	Stage 1 25'/sec	Stage 1 50'/sec	Stage 2 12.5'/sec	Stage 3 12.5'/sec
1	16.0	56.6	0	8.4
2	63.0	75.5	71.2	23.6
3	77.4	86.8	73.6	48.5
4	85.3	91.8	81.0	65.5
5	90.0	94.2	88.4	79.0
6	92.7	95.3	91.9	88.0
7	94.1	95.9	94.1	
8	95.0		95.4	93.0
9	96.8		96.3	
10	97.0		96.8	95.0

Note: These predictions are based on Ranz and Wong's[2] experimental data and on the assumption that mixing is complete.

In general, it can be seen that the theoretical method of efficiency prediction is quite informative and is certainly of value in pointing out the relative merit of various types of packing and the effect of air velocity. The accuracy of the predictions has been validated by several experimental studies on the collection of liquid drops on single collectors although at the time this program began there were no experimental data on the collection of solid particles by multiple elements. Although there seemed to be little doubt that solid particles would behave in the same fashion as liquid drops, the relationship between the behavior of single collector elements and groups of elements had not been established nor was the effect of the scrubbing liquid known.

An experimental program for the study of fluid-flow characteristics and collection efficiency of fibrous packed sections was initiated. At the time when the pressure-drop and flooding-point runs on various sizes of steel

wool had been completed and collection-efficiency tests were beginning, a paper on the collection efficiency of water-washed metal wool was presented by R. G. Calkins.[1] That investigation involved the experimental determination of collection efficiency for two different grades of metal wool and three different types of dust. The data showed that the collection efficiency can be predicted with an average error of about 2% (high) and a maximum of 5% (high). It was found that the flow rate of the scrubbing liquid (water) had little or no effect on the collection efficiency so long as there was sufficient flow to wash the fibers clean.

This information was quite helpful, although there remained one point which was not completely settled. That was the relationship between the behavior of a single collector wire and the behavior of a group of wires. While Calkins' data can yield an answer on this point, it is only a partial answer since he made experimental determinations with fibers which had a triangular cross section and based his predictions on cylindrical collectors with an "equivalent diameter." Consequently, our experimental program was directed toward the investigation of beds of cylindrical wires so that the effect of irregular collector cross section would be eliminated.

Experimental work with silica dust and oil-washed wires showed:

1. The dust collection efficiency of fibrous packing can be predicted to within an average of 2 percent, except for knitted-mesh-type packing, for which the predictions were as much as 7 percent high.

2. The assumption of no mixing of the air stream within the bed appears to be the most suitable.

3. The collection efficiencies predicted by Langmuir and Blodgett give the best agreement.

These conclusions are questionable for collection of dust on dry wires as shown by Interim Technical Report No. 6 (Appendix C). The method is adequate for the prediction of efficiency for deep, dense beds of wetted fibers, but it is considerably in error for shallow, low-density beds. With the data at hand it is not possible to go much further than this toward either evaluating or refining the method. The crucial point seems to be whether the collisions of particles with collectors will be effective or whether there will be an appreciable amount of bouncing-off.

Pressure drop for air flow through beds of fibers can be predicted by the following equation if the distance between fibers is at least 8 fiber diameters:

$$\Delta P = \frac{C_D \, v^2 \, \rho_B \, \rho_G \, L}{\pi \, \rho_W \, r_W \, g_c} \quad ,$$

where

ΔP = pressure drop (lb/ft^2),

v = air velocity (lb/sec),

ρ_B = bed density (lb/ft^3),

ρ_G = gas density (lb/ft^3),

L = bed length (ft),

π = 3.1419,

ρ_W = fiber density (lb/ft^3),

r_W = fiber radius (ft),

g_c = 32.2 (ft/sec^2), and

C_D = drag coefficient for packing fibers.

The application of this relationship to the prediction of pressure drop for air flow through beds of round steel wire is shown in Fig. 4 (Fig. 10 in I.T.R. 3). No data are available to evaluate the effect of the interaction of flow patterns around fibers for dense beds. An empirical relationship defining pressure drop for air flow through beds of steel wool was developed as follows:

$$\frac{\Delta P''}{L\rho_B'} = 0.021 \frac{v^{1.7}}{R_D^{0.5} D_W^{1.1}},$$

where

$\Delta P''$ = pressure drop (inches of water),

L = bed length (ft),

ρ_B' = bed density (gm/cm^3),

v = superficial linear velocity (ft/sec),

R_D = ratio of wire spacing to wire diameter,

D_W = wire diameter (inches), and

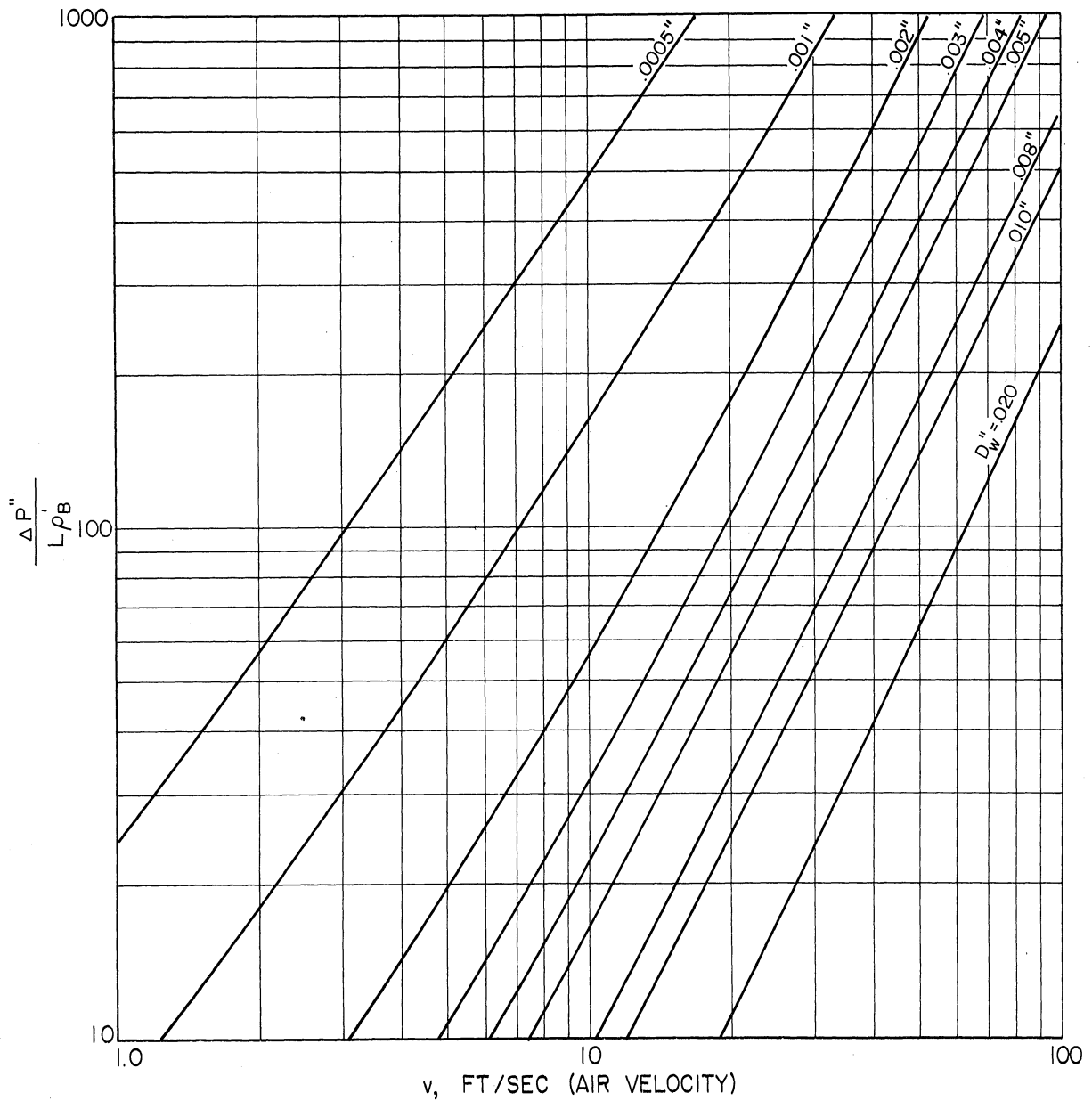d = wire spacing = $r_W \sqrt{\dfrac{\pi\rho_W}{\rho_B}}$.

Fig. 4. Predicted pressure drop group vs air velocity for air flow through beds of round steel wire.

Based on:

$$\frac{\Delta P''}{L\rho'_B} = 2.2 \times 10^{-4} \; C_D \; \frac{v^2}{r''_w} = \frac{'' H_2O}{ft \times gm/cc}$$

$$(\rho_{air} = .075 \; lb/cu \; ft, \; \mu_{air} = .018 \; CP).$$

The $\underline{flooding}$ $\underline{point}$ of a packed column is the gas rate at which liquid is blown out of the column when it is operated at a particular liquid rate. It is therefore an upper limit on allowable gas velocity for any particular liquid flow rate. Experimental data on the flooding of steel-wool and copper-wire packing were correlated by an extension of the Sherwood correlation for packed columns.[3] This correlation is shown in Fig. 5 (Fig. 14 of I.T.R. 3). The definitions of the symbols used in the correlating groups are as follows:

u_O = superficial gas velocity (ft/sec),

S = surface area of packing per cubic ft of column volume (ft^2/ft^3),

g = 32.2 (ft/sec^2),

F = fraction voids (ft^3/ft^3 of tower),

ρ = density (lb/ft^3),

μ = viscosity of liquid (centipoise),

L = superficial liquid mass velocity ($lb/sec/ft^2$), and

G = superficial gas mass velocity ($lb/sec/ft^2$).

The direct application of the flooding-point correlation to the problem of flooding in oil-bath air cleaners cannot be made without knowing the relationship between liquid holdup and the flow rates. Liquid holdup in an air cleaner is determined by the amount of oil which can be blown out of the baffle cup. Flooding points for an air cleaner should thus be stated in terms of the air rate which causes flooding for a given quantity of holdup per volume of packing.

TEST METHODS

The subject of test methods for determining dust collection efficiency was covered in Interim Technical Report No. 2. The following is reproduced from that report:

"After several months of study it became apparent that the biggest deterrent to rapid progress in the experimental testing and evaluation of air cleaners was the lack of a satisfactory dust collection efficiency test. The method widely used by air-cleaner manufacturers and the Detroit Arsenal consists of dispersing A. C. test dust in air, feeding the resulting suspension to an air cleaner, and filtering the entire effluent stream through Canton flannel. The collection efficiency is determined from the weight loss of the
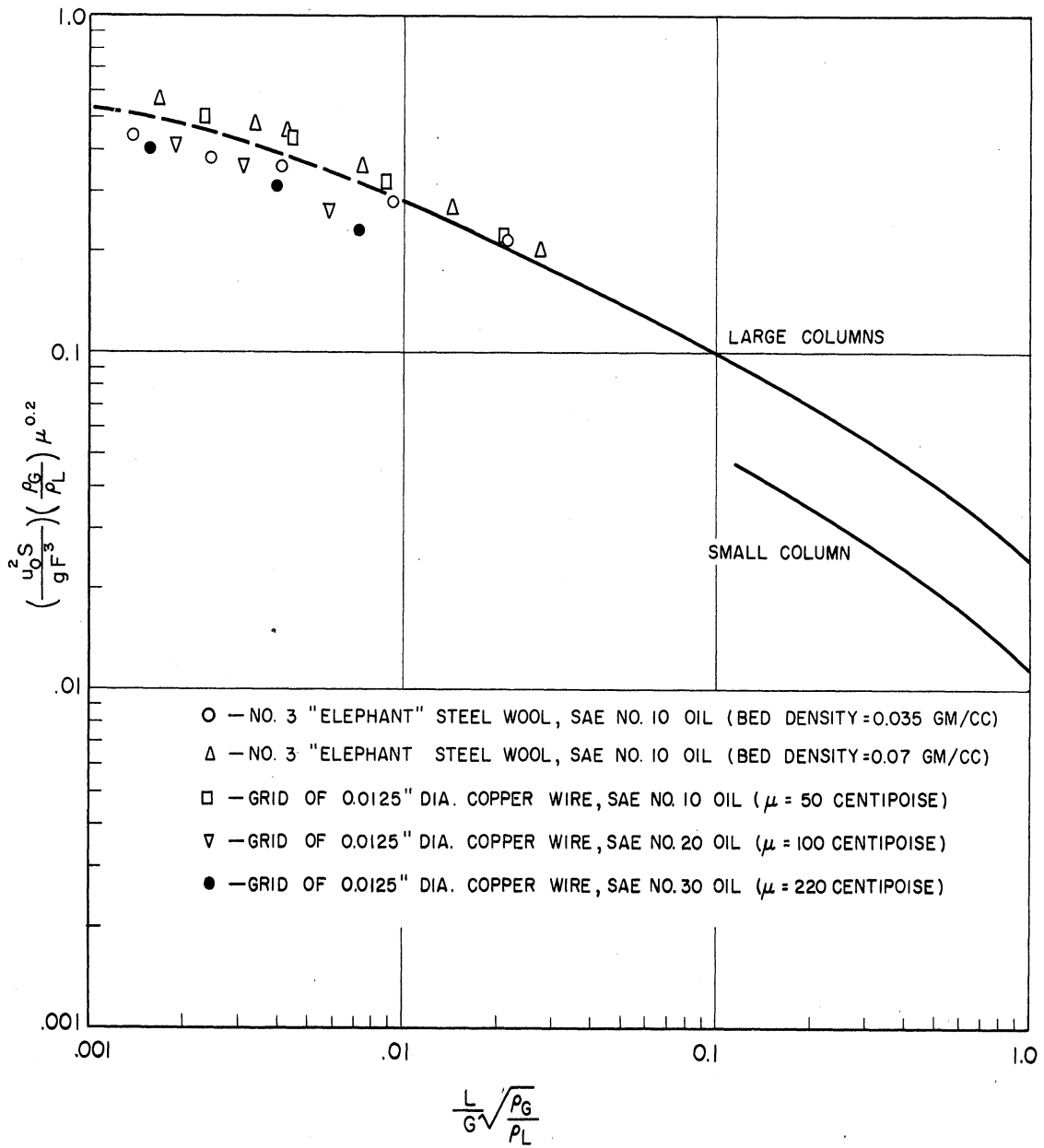
Fig. 5. Flooding-point correlation for fibrous packing.

The y-axis is labeled $\left(\dfrac{u_o^2 S}{g F^3}\right)\left(\dfrac{\rho_G}{\rho_L}\right)\mu^{0.2}$ and the x-axis is labeled $\dfrac{L}{G}\sqrt{\dfrac{\rho_G}{\rho_L}}$.

LARGE COLUMNS

SMALL COLUMN

O — NO. 3 "ELEPHANT" STEEL WOOL, SAE NO. 10 OIL (BED DENSITY = 0.035 GM/CC)

△ — NO. 3 "ELEPHANT STEEL WOOL, SAE NO. 10 OIL (BED DENSITY = 0.07 GM/CC)

□ — GRID OF 0.0125" DIA. COPPER WIRE, SAE NO. 10 OIL (μ = 50 CENTIPOISE)

▽ — GRID OF 0.0125" DIA. COPPER WIRE, SAE NO. 20 OIL (μ = 100 CENTIPOISE)

● — GRID OF 0.0125" DIA. COPPER WIRE, SAE NO. 30 OIL (μ = 220 CENTIPOISE)

dust feeder and the weight gain of the "absolute" filter. There are several drawbacks to this method.

"First, the dust feeders employed do not completely de-agglomerate the test dust. As a result, the dust dispersion product has a larger mean particle size than the size analysis of the A. C. dust indicates and the efficiency of the air cleaner is higher than it would be for a true dispersion of the test dust. This is indicated by the fact that a precleaner attached to an oil-bath air cleaner causes the combined efficiency to be lower than that for the oil-bath cleaner alone. Also, passing the dust-laden air from a "stoker" type dust feeder through an air jet ejector causes the collection efficiency of an oil-bath air cleaner to drop from around 98 percent to the range of from 60 to 80 percent. Since the effect of both the precleaner and the ejector is to break up agglomerates (little or no primary grinding occurs), it is obvious that the original test dispersion contained an appreciable quantity of agglomerates of small particles.

"Second, the absolute filters are quite troublesome to use since they must be large (because of their pressure drop and efficiency limitations) and will absorb moisture. Considerable time is expended in running a test long enough to collect a weighable quantity of dust on the filter, dismantling and drying the filter cloth, and in weighing the cloth and filter holder. Because the filter is so large, an abnormally large analytical balance must be used in order to accurately determine its weight.

"Third, the range of efficiency obtained with the incompletely dispersed A. C. test dust is so high that variations in air-cleaner performance are reflected by changes in efficiency of about one percent and are consequently hard to detect. Another disadvantage of the high efficiency range is that any sort of filtering or sampling process performed on the effluent air must be carried out for a long time in order to collect enough dust to weigh.

"The situation may be summarized by stating the requirement which a good test method would fulfill. These requirements are as follows:

1. The test dust should be completely dispersed and agglomerate-free so that its actual particle-size distribution in suspension is known.

2. The particle-size distribution of the test dust should be such (i.e., small enough) that the efficiency of a standard air cleaner will be approximately 50 percent and changes in air-cleaner design and performance will cause appreciable variations in collection efficiency.

3. The method for determining the dust concentration in the inlet and outlet air should be accurate and rapid and, if possible, should provide a continuous record of instantaneous readings.

The time required for an efficiency test should be no longer than about 10 minutes.

"POSSIBLE IMPROVED TEST METHODS

"Quite a few methods can be conceived, many of which have been reported in the literature, which offer promise for meeting the requirements for a good collection efficiency method. The basic points of these methods may be classed as methods of dispersal, methods of sampling, and methods of aerosol analysis without sampling. Among the methods of dispersal are the redispersal of a powder in air, the spray drying of a solution containing a dissolved solid, the condensation of a vapor to form liquid droplets, and the formation of liquid droplets by atomization. While the employment of liquid drops has some advantages, it was considered more appropriate to employ solid particles for the testing of oil-bath cleaners since their retention in the cleaner is partially dependent on their being wetted by the oil. Some sampling methods suitable for this application are wet collection (preferably of a soluble dust), electrostatic precipitation, thermal precipitation, and filtration with a millipore filter. All of these methods would be applied to the separation of dust from a small sample of the total air stream. To insure that the sample be representative it would have to be taken under isokinetic conditions; that is, the velocity into the sample tube must match the local velocity of the main air stream. While the last three methods listed are capable of very high collection efficiency, they all require the disassembly of apparatus and the removal of the captured sample for weighing. The first method listed is not quite as efficient as the others, but it possesses the attractive feature of being capable of continuously dissolving the dust in a solution whose properties can be measured.

"The principal methods of analysis without sampling involve the application of light-scattering measurements or the use of radioactive tracers as test dust. Both methods have the advantage that they can continuously monitor a flowing stream without having to collect the suspended material.

"THE EVALUATION OF PROPOSED TEST METHODS

"While there was not sufficient time available under the present contract to fully explore and develop the possibilities for improved collection efficiency test methods, it was considered worth-while to briefly study and evaluate the most promising. The processes chosen for study were methods of redispersing powders in air, the spray drying of a salt solution, the analysis of a salt-dust suspension by means of a wet-collection device, the application of light-scattering techniques to aerosol analysis, and the use of radioactive test dust. The investigation of powder dispersal is still in progress and will be reported later. The evaluations of the remaining processes are presented in this report and may be summarized as follows:

1. Spray drying is a feasible process for the preparation of a suspension of salt particles suitable for air-cleaner testing. An experimental investigation of the characteristics of the dust produced by drying an air-atomizing spray indicated that a suitable quantity of dust ranging in size from 0 to 10 microns can be produced with simple apparatus. The maximum size of the particles can be controlled as desired by the proper design and operation of the apparatus.

2. The continuous analysis of a salt-dust suspension can be accomplished by the combined use of a wet-collection device and apparatus for measuring the electrical conductivity of the collecting liquid. Several collection devices were tested, and it was shown that both wet impingers and fiber-packed scrubbers are suitable. This type of device could be applied to the analysis of either a sample of the air stream or the entire stream.

3. Light-scattering techniques offer considerable promise as a rapid analytical method. The properties of a light-attenuation system were predicted by means of computations based on light-scattering theory as applied to a representative test dust (silica). It is shown that the method is capable of about 1/2- to 1-percent accuracy in collection efficiency determination and that it is most sensitive to the smaller particles. The measurement of forward scattering is another possibility along this line and could result in an even more sensitive method.

4. The use of a radioactive tracer as a test dust or as an additive to test dust would be feasible and would offer no great problem in protection from radiation. The most suitable tracers would be phosphorous 32 and sulfur 35, which are both beta emitters. The employment of Geiger counters as monitors on the inlet and outlet streams from an air-cleaner would permit the determination of collection efficiency to about 2- to 5-percent accuracy. Since the tracers have short half-lives, the disposal of sludge, etc., would be safe after a retention period of a few weeks.

"A comparative evaluation of these methods leads to the recommendation that light-scattering techniques be the first choice for development as a routine analytical method. The second choice would be the use of a spray-dried salt dust and the wet-collection plus conductivity measurement analytical system. The use of radioactive tracers is not recommended as a routine test method because of the complexities of scheduling and the safety precautions required."

CHAPTER III

CONCLUSIONS

As a result of the work done on this program it is apparent that oil-bath air cleaners can be designed on the basis of engineering considerations. Performance can be predicted within reasonable accuracy even though there remain some areas of doubt and some relationships still to be determined. Certainly the relative merits of alternative designs can be evaluated with considerable reliability even though absolute magnitudes might be in error. Our interviews with air-cleaner manufacturers pointed out the importance of stressing this point since at least up to 1955 there was practically no application of science to the design of commercial engine air cleaners.

Specifically, the situation at present is as follows:

1. Dust collection efficiency can be predicted with acceptable accuracy for wetted systems although results on dry wires indicate that the subject is not completely understood. Further work is required.

2. Pressure drop can be predicted with acceptable accuracy and indications are that considerable improvement (lowering of pressure drop) could be attained through design changes.

3. A rough indication of flooding point (or carry-over limit) may be predicted but further work must be done to relate it to liquid holdup.

4. Present collection-efficiency test methods are not satisfactory and more promising methods are known which could be developed.

REFERENCES

1. Calkins, R. G., "Filter Scrubber Dust Collectors," Presented at the American Chemical Society Annual Meeting in New York, September, 1954.

2. Ranz, W. E. and Wong, J. B., "Impaction of Dust and Smoke Particles," Ind. Eng. Chem., 44, 1371 (1952).

3. Sherwood, Shepley, and Holloway, "Flooding Velocities in Packed Columns," Ind. Eng. Chem., 30, 765 (1938).

Theoretical Values of the Coefficient of the
Pressure Loss in the Cup Region of the Test Apparatus

The theoretical values of C_L are calculated in Table III using Equation (23)

$$C_L = \left[\frac{1}{C_c} - \frac{1}{\left(\frac{D}{d}\right)^2 - 1} \right]^2 , \qquad (23)$$

where

$$C_c = b/a \qquad (34)$$

$$b/a = f\,(c/a) \qquad (\text{Fig. 17}) \qquad (35)$$

$$c/a = 4\,(h/d) \qquad (29)$$

which in effect specify the following relation for the test apparatus.

$$C_L = f\,(h/d,\ D/d) \qquad (36)$$

giving theoretical values of C_L which are plotted as dashed lines in Fig. 13. The experimental values of C_L in Fig. 13 are seen to agree with the theoretical values within limits which are quite satisfactory for air cleaner design purposes.

Having verified the formula (23) for C_L, a completely theoretical expression for the pressure drop in the cup region of the oil spray test apparatus may be written. Substituting (23) in (16),

$$K = 1 - \left[\frac{1}{\left(\frac{D}{d}\right)^2 - 1} \right]^2 + \left[\frac{1}{C_c} - \frac{1}{\left(\frac{D}{d}\right)^2 - 1} \right]^2 \qquad (37)$$

where, by (8) and (10a),

$$\Delta P \quad = \quad p_1 \; - \; p_4 \quad = \quad 1/2(\rho \; V_1{}^2)K \qquad\qquad (38)$$

$$V_1 \quad = \quad Q/A_1 \quad . \qquad\qquad\qquad (39)$$

Experimental Values of the Pressure Drop in
the Baffle Region of a Production Model Air Cleaner

        Figure 11 presents a sectional view of the axially symmetric Donald-
son 410-cfm air cleaner. The static gage pressures were measured for a range
of flow rates up to 400 cfm at points indicated by circled numbers. This
section is concerned with the pressure drop in the baffle region as indicated
by the measurements at points a, b1, and b2. Figure 18 shows an enlarged view
of the baffle region and also the general character of the flow in this region
as observed in model tests.

        The experimental values of K corresponding to the pressure drop in
the baffle region are calculated in Table IV and plotted in Fig. 19 as solid
lines. The presence of oil in the air cleaner is seen to have a negligible
effect on the drop in the baffle region. The relatively constant value of K
at the higher flows indicates that the rates of flow in the baffle region are
sufficiently high so that Reynolds' number is not a factor.

Theoretical Values of the Pressure Drop
in the Baffle Region of the Air Cleaner

        In Fig. 18 the velocity is known to be essentially uniform over the
cross sections of 1 and 2 for the same reasons as given for the corresponding
points of the test apparatus. The flow leaving the first screen was observed
to be uniform in the water channel tests of two-dimensional models. Conse-
quently, the velocity V_4 is taken as uniform over the upstream surface of the
first screen. Specifically, the velocity V_4 is assumed to be uniform over an
area A_4 consisting of the total area of the stream as it passes through the
upstream (first) layer of the screens comprising the first screen region.
Station 4 is taken in the first layer since this is the only point of the
main stream in this locality at which a uniform velocity distribution is
likely. The pressure measured at point b2 (or b1) is assumed to have the same
value as p_4, a constant pressure over the area A_4.

The formula for the pressure drop between 1 and 4 may be obtained in the manner demonstrated above in the analysis of the test apparatus.

$$K = \frac{p_1 - p_4}{1/2(\rho \, v_1{}^2)} = \left[1 - \left(\frac{A_1}{A_2}\right)^2 \right] + C_L \qquad (40)$$

The pressure-loss formula (20) will also apply:

$$p_L = 1/2(\rho \, v_1{}^2) \, (A_1/A_2 - A_1/A_4)^2 \; ; \qquad (20)$$

and since C_L is defined by (11) as

$$p_L = C_L \, (1/2\rho \, v_1{}^2) \, , \qquad (41)$$

we have

$$C_L = \left(\frac{A_1}{A_2} - \frac{A_1}{A_4}\right)^2 = \left(\frac{1}{C_c} - \frac{A_1}{A_4}\right)^2 \, , \qquad (42)$$

where C_c is still determined by Fig. 17 and the set of equations [(34), (35), and (29)] which are listed together on page 9. Then (40) becomes

$$K = \left[1 - \left(\frac{A_1}{A_4}\right)^2 \right] + \left[\frac{1}{C_c} - \frac{A_1}{A_4} \right]^2 \, . \qquad (43)$$

If $A_4{}'$ is the gross annular area of the first screen region (the area at 4 which is open to flow if the screens of the first region are removed), and if C_4 is the fraction of $A_4{}'$ which is open (i.e., which is not occupied by the wire of the first layer of screen, the area open to flow in this layer is $C_4 A_4{}'$. If, then, C_{c4} is the coefficient of contraction of the portion of the stream through any one opening of the first layer, the area of the total stream at station 4 is

$$A_4 = C_{c4} \, C_4 A_4{}' \qquad (44)$$

and

$$\frac{A_1}{A_4} = \frac{1}{C_{c4}\, C_4}\left(\frac{A_1}{A_4'}\right)\ . \tag{45}$$

Utilizing the area theorem of Pappus* to determine A_4', we obtain

$$\frac{A_1}{A_4'} = \frac{d^2}{(2/\sqrt{3})(D_a{}^2 - D_d{}^2)} = \frac{\sqrt{3}}{2}\left[\frac{1}{\left(\frac{D_a}{d}\right)^2 - \left(\frac{D_d}{d}\right)^2}\right]\ , \tag{46}$$

which for the dimensions of Fig. 18 becomes

$$\frac{A_1}{A_4'} = 0.211\ . \tag{47}$$

In the Donaldson 410-cfm air cleaner, the first screen region consists of layers of 14-mesh screen of 0.0165-in.-diameter wire. For this material, C_4 is readily computed to be

$$C_4 = 0.5914\ . \tag{48}$$

The coefficient of contraction C_{c4} is given with sufficient accuracy by that for a sharp edge, circular orifice in a round pipe. The coefficient for the latter case is essentially the discharge coefficient plotted in Fig. 20** against the square root of the Reynolds' number with the ratio of orifice diameter to pipe diameter as a parameter. For the flow through the first layer of the first screen region the value of this parameter may be taken as

$$\frac{k}{m} = \frac{m - n}{m} = \frac{0.0714 - 0.0165}{0.0714} = 0.77 \tag{49}$$

*Mechanical Engineers' Handbook, L. S. Marks (editor), 4th edition, 1941, p. 111 (listed as the second theorem of Pappus in this reference).

**H. Rouse, Fluid Mechanics for Hydraulic Engineers, First Edition, McGraw-Hill Book Company Inc., New York, 1938, p. 260.

where m is the distance between the axes of parallel wires, n is the wire diameter, and k is the length of a side of an individual square opening in the screen. The Reynolds' number may be estimated as

$$R = \frac{V_4\, k'}{v} = \frac{4Q}{\pi(k')^2}\frac{k'}{v} \cong \frac{4Q}{\pi k v} \qquad (50)$$

where k' is the diameter of a circle of area k^2. If

$$Q = 100\ ft^3/min = (100/60)\ ft^3/sec\ ,$$

$$k = 0.0714 - 0.0165 = 0.0549\ in. = 0.0549/12\ ft,\ and$$

$$v = 18.5 \times 10^{-5}\ ft^2/sec \quad \text{(kinematic viscosity for air}$$
$$\text{at } 60°F \text{ and } 29.5" \text{ Hg) },$$

then

$$R = 2,509,000 \text{ at } 100 \text{ cfm} \qquad (51)$$

and

$$\sqrt{R} = 1,548 \text{ at } 100 \text{ cfm.}$$

This high value of R at only 25 percent of the maximum flow indicates (Fig. 20) that C_{c4} is independent of the Reynolds' number. Using the value in (49), and consulting the portion of Fig. 20 corresponding to high values of R,

$$C_{c4} \cong 0.63\ . \qquad (52)$$

Substituting (47), (48), and (52) in (45),

$$\frac{A_1}{A_4} = \frac{1}{(0.5914)\,(0.63)}\,(0.211) = 0.566 \qquad (53)$$

and

$$\left(\frac{A_1}{A_4}\right)^2 = 0.321\ . \qquad (54)$$

From the dimensions of Fig. 18, we obtain

$$h/d = 0.36 \tag{55}$$

whence by (29)

$$c/a = 4(h/d) = 1.44 \tag{56}$$

and by Figure 17

$$C_c = b/a = 0.663 , \tag{57}$$

so that

$$1/C_c = 1.51 . \tag{58}$$

Then substituting (53), (54), and (58) into (43),

$$K = (1 - .321) + (1.51 - .566)^2 = 1.56 . \tag{59}$$

This computed value of K is plotted as a dashed line in Fig. 19 where, at the higher flows, it can be seen to be in essential agreement with the experimental values. Equations (42) and (43) originally derived for the test apparatus, are now verified for the air cleaner.

Minimum Pressure Loss in the Baffle Region

For the test apparatus, use was made of the relation

$$\frac{A_1}{A_4} = \frac{\pi/4 \; d^2}{\pi/4 \; (D^2 - d^2)} = \frac{1}{(D/d)^2 - 1} . \tag{60}$$

To permit comparison of C_L for the test apparatus and air cleaner, let (60) define D/d in the latter case. Thus, by (53) and (60)

$$0.566 = \frac{1}{\left(\frac{D}{d}\right)^2 - 1} \tag{61}$$

and

$$(D/d)^2 = 2.767, \quad D/d = 1.663 . \tag{62}$$

Using this value of D/d, the theoretical value of the loss coefficient C_L of the cleaner is calculated from Equation (42) as a function of h/d (Table V) and plotted in Fig. 21. The value of C_L for the present design of the baffle region is, according to Equation (55), that corresponding to $h/d = 0.36$. That is, $C_L = 0.89$. The theoretical values of C_L for other values of D/d are also plotted in Fig. 21 and have been taken from Fig. 13.

Comparing the experimental values of C_L in Fig. 13 for the test apparatus, we see that the data suggest the existence of minimum values of C_L for certain values of h/d. By Equation (43) these points will correspond to the minimum possible values of K, and thus of the pressure drop, for a given value of A_1/A_4 (i.e., of D/d). The experimentally determined minimum values of C_L are plotted against D/d in Fig. 22.

From Equation (42) it can be seen that the minimum value of C_L will correspond to a maximum value of C_c which approaches the limit unity as h/d (that is, c/a) increases in Fig. 17. These theoretical minimum values of C_L are calculated in Table VI and are plotted in Fig. 22 against the ratio D/d representing the range of A_1/A_4 of interest.

It is apparent from Fig. 21 that the value of $C_L = 0.89$ for the present design of the air-cleaner baffle region will decrease rapidly as h/d is increased above its present value of 0.36. A further improvement will result (Fig. 22) from decreasing the ratio D/d, that is, from increasing the value of A_1/A_4, if practicable.

Distribution of Pressure Drop and Flow in
Various Regions of the Donaldson Air Cleaner

The pressure was measured at seven stations in the Donaldson 410-cfm
air cleaner (Fig. 11) for various air flow rates with and without oil in the
cleaner. When oil was present in the cleaner, the manometer connection was
tied into a bubbler, and an extremely low rate of air flow was allowed to pass
through the manometer tap into the air cleaner. The bubbler permitted obser-
vation of the flow and thus a continuous check against plugging of the line by
oil. There was no indication of plugging at any time and, as shown in Fig. 23,
pressure drops measured with oil present agreed well with measurements made in
the absence of oil except in the main screen region where such agreement was
not to be expected.

Table VII summarizes the pressure measurements obtained. Table VIII
gives the pressure drops in the entry, baffle, main screen, and discharge
regions of the cleaner, as computed from the pressure measurements of Table
VII. In the following discussion, attention is devoted primarily to the
maximum pressure drops (occurring at the maximum flow), since these are an
important factor in design.

Effect of Oil on Pressure Drop

The average pressure drops in the various regions are plotted in
Fig. 23. At the larger flows where the higher pressure drops are encountered,
the data covers tests both with and without oil. At the maximum flow, the
presence of oil is seen to have a significant effect on pressure drop only in
the main screen region where it causes an increase of 500 percent. The
corresponding increase of pressure drop in the baffle region is only 12 percent.

Comparison of Pressure Drop in Various Regions

In Fig. 23 it is seen that, in the presence of oil and at maximum
flow, the pressure drops are about equal in the baffle, main screen, and dis-
charge regions. However, the drop in the entry region is much larger and, in
fact, is 4.8 inches of water or about 60 percent of the total drop through the
cleaner.

The pressure drop in the baffle region has been analyzed above. The pressure drop in the main screen and discharge regions is discussed below in connection with the circumferential distribution of flow.

The large drop in the entry region was anticipated from the study of two-dimensional models in the water channel. As noted in Chapter III, the drop in the entry region can be substantially reduced by the addition of a ring-type vane to divert flow through the space at the upper end of the down tube, which is now occupied by an elongated toroidal eddy. This change may be effected as a modification of the present design of the entry region, but a redesign of this region may be preferable from a manufacturing standpoint. In either case, it appears that the present entry baffle may remain unchanged if so desired.

Circumferential Distribution of Flow

As can be seen in Fig. 11, the pressure-measurement stations in the Donaldson air cleaner were selected so as to obtain an indication of the amount of non-uniformity in the distribution of the air flow around the axis of the cleaner. The pressure drops with oil present are plotted in Fig. 24 for both the outlet side of the cleaner (side 1) and the opposite side (side 2).

The flow on the two sides appears to be quite uniform except in the discharge region, where a marked non-uniformity appears to exist. Here the pressure drop on side 1 is seen to exceed that on side 2 by a factor of 10. This condition indicates that in the discharge region the flow on side 1 may be more than 3 times that at 2, since the average drop in this region varies approximately as the square of the rate of air flow. Such a non-uniformity would represent a considerable overloading of the screen in the discharge region near side 1 and underloading elsewhere in this region.

In the present design, the outlet restriction has been intentionally varied around the discharge region, decreasing from side 1 toward side 2. Also, a top view of the cleaner would show that the centerline of the outlet nipple of the air cleaner is not located in a radial plane of the air cleaner, but is eccentric, presumably in order to induce in the outlet manifold a unidirectional circulatory flow about the axis of the cleaner. The varying restriction and eccentric outlet should promote uniformity of flow in the discharge region. However, it appears that they are inadequate for this purpose, at least as now incorporated in the design of the cleaner.

Presumably, a more uniform flow could be obtained by adopting a more drastic variation of the outlet restriction from side 1 to 2, even at the expense of increasing the average pressure drop in the discharge region.

Furthermore, any increase in pressure differential may be more offset by the proposal for decreasing the drop in the entry region. An alternative and preferable solution may lie in moderately increasing the variation of the outlet restriction and also effecting a general re-shaping of the outlet manifold which as now designed is not conductive to a stable pattern of the flow within it. It may also be necessary to restrict circumferential flow in the screen of the discharge region by some means such as that described next.

It is assumed that the placing of vertical guide vanes at various radial positions in the discharge region is undesirable from a manufacturing standpoint. In the case of the Donaldson air cleaner, the screen in this region consists of 26 turns of crimped, 12-mesh screen of 0.0105-inch-diameter wire. This screen differs from that used elsewhere in the cleaner. By virtue of the observed non-uniformity which exists solely in the discharge region, the screen used here must permit considerable circumferential flow as the air stream approaches the outlet restriction. Since this tangential component of flow is not of the unidirectional, circulatory type apparently intended, a different type of screen in the discharge region which discourages all circumferential flow may give improved results. Such a screen would act in the same manner as radial guide vanes without introducing the practical problems caused by the latter. In this manner, the uniform flow now existing in the baffle and main screen regions (Fig. 23) would tend to persist in the discharge region.

Conclusions

The study of the cup region of the test apparatus and the baffle region of the Donaldson 410-cfm air cleaner provides some insight into the behavior of the air flow in these sections. The theoretical equation (38) is shown (Fig. 13) to adequately relate the pressure drop, the rate of flow, and the dimension ratios (h/d and D/d) of the test apparatus for a considerable range of the latter ratios. The equation is also shown (Fig. 19) to be applicable, at the higher rates of flow, to the baffle region of the Donaldson cleaner. In view of this verification over a considerable range of size and form of the flow boundaries, Equation (38) can be expected to apply to the corresponding region of other sizes and models of air cleaners.

The application of these results to baffle region design is then illustrated for the Donaldson cleaner. It is shown that in the case of this cleaner the coefficient of pressure loss, C_L, can be decreased considerably by increasing (h/d) slightly (Fig. 21) and also, if practical, by decreasing (D/d) (Fig. 22). In general, if one of the set of dimensions h, d, or D (or the equivalent set h, A_1, and A_4) is specified, the analysis provides a guide

in selecting the values of the others which will yield a minimum pressure loss in the baffle region.

To illustrate a method of analyzing other regions of an air cleaner, attention is then given to the distribution of the pressure drop and flow in the various regions of the Donaldson air cleaner, as indicated by pressure measurements at various points in the cleaner. The following conclusions are indicated by the data:

1. The relation between the average pressure drop and the rate of air flow is essentially unaffected by the presence or absence of oil in the cleaner except in the main screen region, where a large effect is observed (Fig. 23). Consequently, an analysis of the air flow in the absence of oil, such as that carried out for the baffle region, would be ineffective in the main screen region but could be expected to be possible for the entry and discharge regions. However, such an analysis in the latter regions offers but limited usefulness, since the various cleaners differ substantially in the geometry of their entry and discharge sections. Furthermore, as noted below, the measures for reducing the pressure drop in these regions can be determined merely by observation of the flow pattern.

2. The average pressure drops in the baffle, main screen (with oil present), and discharge regions are about equal (Fig. 23). Consequently, the possible reductions in the baffle pressure drop already noted (Figs. 21 and 22), would permit increasing the density of wire in the main screen region, if desired, without increasing the overall pressure drop in the cleaner.

3. The average pressure drop is largest in the entry region (Fig. 23) where it is about 60% of the total drop through the cleaner. Means for reducing this drop are suggested by the study of the photographs of the flow in the entry region and are discussed in this chapter.

4. The pressure-drop measurements on the outlet side (side 1) of the cleaner and on the opposite side (side 2) are plotted in Fig. 24. The data indicate that the flow in the baffle and main screen regions is of uniform circumferential distribution, but the flow on side 1 of the discharge region is several times that on side 2. Several possible solutions have been suggested in this chapter.

In general, the analytical study proved desirable in some regions and not in others. However, it is seen that in a problem with abrupt changes in the dimensions of the flow boundaries, such as in the air cleaner, it is always necessary to have advance knowledge of the general shape of the main air stream and eddy regions whether or not an analytical study is made. With

experience, the stream and eddy pattern can be predicted in simple cases, but in general such a procedure is unreliable. It is also unnecessary to attempt predictions of this kind in view of the ease and effectiveness with which the water channel and two-dimensional models can be used to study the flow pattern. The study of air cleaner models in the water channel is described in Chapter III of this report.

TABLE I

EXPERIMENTAL VALUES OF THE PRESSURE DROP IN THE TEST APPARATUS

$$K = \frac{\Delta P}{\frac{1}{2}\rho V_1^2} \quad ; \quad \Delta P = P_1 - P_4$$

① Item	② D/d	③ h/d	④ Ah/A1 (4h/d)	⑤ A4/A1 $(\frac{D}{d})^2-1$	⑥ Ah/A4 ④/⑤	⑦ ΔP (in. H₂O)	⑧ Q (scfh)	⑨ K	⑩ Reg. No. (Q/d) (ft²/sec)	⑪ H/d	⑫ h/H ③/①	⑬ l/d	⑭ d (in.)
1	2.00	.125	.500	3.000	.1665	13.20	4,000	7.01	8.89	1.33	.0938	14.00	1.50
2		.333	1.333		.4439	1.07		5.68			.250		
3		.500	2.000		.6660	−.08		−.042			.375		
4		.916	3.664		1.220	.49		−.263			.687		
5		1.000	4.000		1.333	.48		−.255			.750		
6		1.250	5.000		1.667	.00		.000			.938		
7	2.22	.111	.444	3.928	.113	8.40	6,000	10.00	8.89	1.11	.100	9.33	2.25
8		.333	1.333		.339	.72		.860			.300		
9		.500	2.000		.509	.16		.191			.450		
10		.611	2.444		.622	.00		.000			.550		
11		.777	3.108		.791	.15		−.179			.700		
12		.833	3.332		.848	.12		−.143			.750		
13		1.000	4.000		1.018	.18		−.215			.901		
14	2.66	.125	.500	6.076	.082	17.75	4,000	9.430	8.89	1.00	.125	14.00	1.50
15		.333	1.333		.219	1.20		.637			.333		
16		.584	2.336		.385	.02		.010			.584		
17		.666	2.664		.438	.10		−.053			.666		
18		.916	3.664		.603	.32		−.170			.916		
19		1.000	4.000		.658	.38		−.202			1.000		
20		1.333	5.333		.878	.11		−.058			1.333		

TABLE I (cont.)

① Item	② D/d	③ h/d	④ Ah/A₁ (4h/d)	⑤ A₄/A₁ $(\frac{D}{d})^2 - 1$	⑥ Ah/A₄ (④/⑤)	⑦ ΔP (in. H₂O)	⑧ Q (scfh)	⑨ K	⑩ Reg. No. (Q/d) (ft²/sec)	⑪ H/d	⑫ h/H (③×⑪)	⑬ l/d	⑭ d (in.)
21	3.33	.125	.500	10.089	.050	20.00	4,000	10.62	8.89	1.66	.0753	14.00	1.50
22		.333	1.333		.132	1.83		.956			.201		
23		.666	2.664		.264	– .02		– .010			.401		
24		1.250	5.000		.496	– .39		– .207			.753		
25		1.416	5.664		.561	– .39		– .207			.853		
26		1.666	6.664		.660	– .30		– .159			1.004		
27		1.750	7.000		.694	– .24		– .127			1.054		

Note: Flowing fluid: Air at 70°F and 29.3 inches Hg.

Flow rates (Q) in scfh (ft³/hr at standard temp. and pressure).

Column 4: Ah is defined as (πdh).

Column 9: K is defined as $(\Delta P / 1/2 \rho V_1^2)$, where ΔP is in lb/ft²

V_1 in ft/sec and ρ in slugs/ft³. For units of col. 7, 8, and 14,

$K = (1.69 \times 10^6) \ d^4 \ (\Delta P / Q^2)$.

Column 10: Q/d is proportional to the Reynolds' No. For the Donaldson cleaner

Q/d = 18.22 ft²/sec at 410 cfm.

TABLE II

EXPERIMENTAL VALUES OF COEFFICIENT OF PRESSURE LOSS IN TEST APPARATUS

$$C_L = K + \left[1 - \left(\frac{1}{\frac{D^2}{d^2} - 1} \right) \right]^2$$

① D/d	② h/H	③ h/d	④ (D/d)²	⑤ ④-1	⑥ 1/⑤	⑦ ⑥²	⑧ 1-⑦	⑨ K	⑩ ⑧+⑨	⑪ Ah/A4
2.00	.0938	.125	4.	3.	.3333	.1111	.8889	7.01	7.899	.167
	.250	.333						.568	1.457	.444
	.375	.500						- .042	.847	.667
	.687	.916						- .263	.626	1.221
	.750	1.000						- .255	.634	1.333
	.938	1.250						.000	.889	1.667
2.22	.100	.111	4.928	3.928	.2546	.0648	.9352	10.00	10.94	.113
	.300	.333						.860	1.795	.339
	.450	.500						.191	1.126	.509
	.550	.611						.000	.935	.622
	.700	.777						- .179	.756	.791
	.750	.833						.143	.792	.848
	.901	1.000						.215	.720	1.018
2.66	.125	.125	7.076	6.076	.1646	.02708	.97292	9.430	10.403	.082
	.333	.333						.637	1.610	.219
	.584	.584						.010	.983	.385
	.666	.666						- .053	.920	.438
	.916	.916						- .170	.803	.603
	1.000	1.000						- .202	.771	.658
	1.333	1.333						- .058	.915	.878
3.33	.075	.125	11.089	10.089	.0991	.0098	.9902	10.620	11.610	.050
	.201	.333						.956	1.946	.132
	.401	.666						- .010	.980	.264
	.753	1.250						- .207	.783	.496
	.883	1.466						- .207	.783	.561
	1.004	1.666						- .159	.831	.660
	1.054	1.750						- .127	.863	.694

TABLE III

THEORETICAL VALUES OF COEFFICIENT OF PRESSURE LOSS IN TEST APPARATUS

$$C_L = \left[\frac{1}{C_c} - \frac{1}{\left(\frac{D}{d}\right)^2 - 1}\right]^2$$

① D/d	② h/d	③ c/a 4 x②	④ C_c (Fig. 8)	⑤ $1/C_c$	⑥ $\left[\left(\frac{D}{d}\right)^2 -1\right]^{-1}$	⑦ ⑤-⑥	⑧ ⑦²
2.00	.125	.500	.27	3.704	.3333	3.337	11.14
	.333	1.333	.63	1.587		1.254	1.573
	.500	2.000	.813	1.230		.897	.805
	.916	3.664	.975	1.026		.693	.480
	1.000	4.000	.985	1.015		.682	.465
	1.250	5.000	.996	1.004		.671	.450
2.22	.111	.444	.26	3.846	.2546	3.591	12.90
	.333	1.333	.63	1.587		1.332	1.774
	.500	2.000	.813	1.230		.975	.951
	.611	2.444	.875	1.143		.888	.789
	.777	3.108	.938	1.066		.811	.658
	.833	3.332	.956	1.046		.791	.626
	1.000	4.000	.985	1.015		.760	.578
2.66	.125	.500	.27	3.704	.1646	3.539	12.52
	.333	1.333	.63	1.587		1.422	2.022
	.584	2.336	.863	1.159		.994	.988
	.666	2.664	.900	1.111		.946	.895
	.916	3.664	.975	1.026		.861	.741
	1.000	4.000	.985	1.015		.850	.723
	1.333	5.333	.997	1.003		.838	.702
3.33	.125	.500	.27	3.704	.0991	3.605	13.00
	.333	1.333	.63	1.587		1.488	2.214
	.666	2.664	.900	1.111		1.012	1.024
	1.250	5.000	.996	1.004		.905	.819
	1.466	5.864	1.000	1.000		.901	.812
	1.666	6.664	1.000	1.000		.901	.812
	1.750	7.000	1.000	1.000		.901	.812

Note:
Column 4: C_c is the value of b/a determined from Fig. 8.
Column 6: Values taken from column 6 of Table II.

TABLE IV

EXPERIMENTAL VALUES OF THE PRESSURE DROP
IN THE AIR CLEANER BAFFLE REGION

$$K = \frac{\Delta P}{\frac{1}{2}\rho V_1^2} \quad , \quad \Delta P = p_1 - p_4$$

①	②	③	④	⑤	⑥	⑦	⑧	⑨	⑩	⑪	⑫
		Orif	Q	Without Oil				With Oil			
D_c/d	h/d	Comb	(scfm)	p_1	p_4	ΔP	K	p_1	p_2	ΔP	K
1.33	.36	I	50	- .12	- .125	.005	.384				
			70	- .19	- .22	.03	1.176				
			100	- .35	- .42	.07	1.344				
			150	- .75	- .91	.16	1.365				
		II	150	- .96	-1.12	.16	1.365	- .91	-1.31	.40	3.413
			200	-1.42	-1.70	.28	1.344	-1.35	-1.80	.45	2.160
			300	-3.04	-3.63	.59	1.259	-2.86	-3.48	.62	1.323
			400	-5.10	-6.18	1.08	1.296	-4.80	-6.00	1.20	1.440

Note:

Column 3:   I and II indicate two different orifice combinations used to measure the air flow over the range of 50 to 400 cfm. A slight overlap error can be seen above, but is not important in this problem.

Columns 5 and 6: p_1 and p_4 are, respectively, the gauge pressure measured at station a and the average of the pressures measured at b1 and b2.

Columns 8 and 12:   For the units of columns 4, 7, and 10, K is given by

$$K = 468\,d^4\,(\Delta P/Q^2) = 192 \times 10^3\,(\Delta P/Q^2) ,$$

where d is in inches (d = 4.5 inches).

All pressures in columns 5, 6, 7, 9, 10, and 11 are in inches of water.

TABLE V

THEORETICAL VALUES OF
COEFFICIENT OF PRESSURE LOSS IN AIR CLEANER

$$C_L = \left[\frac{1}{C_c} - \frac{A_1}{A_4} \right]^2$$

① D/d	② h/d	③ c/a 4 x②	④ C_c Fig.8	⑤ $1/C_c$	⑥ A_1/A_4	⑦ ⑤-⑥	⑧ ⑦²
1.66	.125	.500	.270	3.704	.566	3.138	9.847
	.333	1.333	.630	1.587		1.021	1.042
	.360	1.440	.663	1.510		.944	.891
	.500	2.000	.813	1.230		.664	.441
	.916	3.664	.975	1.026		.460	.212
	1.000	4.000	.985	1.015		.449	.202
	1.250	5.000	.996	1.004		.438	.192

TABLE VI

THEORETICAL MINIMUM VALUES C_L
FOR TEST APPARATUS AND AIR CLEANER

$$C_L = \left[\frac{1}{C_c} - \frac{A_1}{A_4} \right]^2 \geqq \left[1 - \frac{A_1}{A_4} \right]^2$$

① D/d	② A_1/A_4	③ 1-②	④ ③²
1.66	.5660	.4340	.188
2.00	.3333	.6667	.444
2.22	.2546	.7454	.556
2.66	.1646	.8354	.698
3.33	.0991	.9009	.812

TABLE VII

EXPERIMENTAL VALUES OF THE PRESSURE AT VARIOUS POINTS
IN THE AIR CLEANER

Sta-tion	Oil	Pressure (inches of water)							
		Orifice Combination I				Orifice Combination II			
		Q = 50	70	100	150	150	200	300	400
a	w/o	.12	.19	.35	.75	.96	1.42	3.04	5.10
b1		.12	.22	.42	.90	1.08	1.70	3.66	6.15
b2		.13	.22	.42	.92	1.16	1.70	3.60	6.20
c1		.15	.25	.45	.95	1.19	1.80	3.80	6.35
c2		.16	.25	.43	.96	1.19	1.75	3.77	6.35
d1		.20	.32	.60	1.25	1.50	2.42	5.10	8.65
d2		.17	.27	.47	1.01	1.22	1.80	3.90	6.45
a	with					.91	1.35	2.86	4.80
b1						1.30	1.77	3.46	6.00
b2						1.32	1.82	3.50	6.00
c1						1.50	2.08	4.20	7.10
c2						1.49	2.07	4.20	7.00
d1						1.85	2.67	5.50	9.20
d2						1.50	2.12	4.28	7.20

Note: All pressures are in inches of water of vacuum below the atmospheric
pressure at the inlet of the air cleaner. Flow rates (Q) are given
in scfm (ft^3/min. of air at standard temperature and pressure).

TABLE VIII

EXPERIMENTAL VALUES OF THE PRESSURE DROP
IN VARIOUS REGIONS OF THE AIR CLEANER

Region	Points	Oil	Pressure Drop (Inches of Water)							
			Q=50	70	100	150	150	200	300	400
Entry	inlet to a	w/o	.12	.19	.35	.75	.96	1.42	3.04	5.10
Baffle	a to bl		.00	.03	.07	.15	.12	.28	.62	1.05
	a to b2		.01	.03	.07	.17	.20	.28	.56	1.10
	average		.00	.03	.07	.16	.16	.28	.59	1.07
Screen	bl to cl		.03	.03	.03	.05	.11	.10	.14	.20
	b2 to c2		.03	.03	.01	.04	.03	.05	.17	.15
	average		.03	.03	.02	.04	.07	.07	.15	.17
Discharge	cl to dl		.05	.07	.15	.30	.31	.62	1.30	2.30
	c2 to d2		.01	.02	.04	.05	.03	.05	.13	.10
	average		.03	.04	.09	.17	.17	.33	.71	1.20
Entry	inlet to a	with					.91	1.35	2.86	4.80
Baffle	a to bl						.39	.42	.60	1.20
	a to b2						.41	.47	.64	1.20
	average						.40	.44	.62	1.20
Screen	bl to cl						.20	.31	.74	1.10
	b2 to c2						.17	.25	.70	1.00
	average						.18	.28	.72	1.05
Discharge	cl to dl						.35	.59	1.30	2.10
	c2 to d2						.01	.05	.08	.20
	average						.18	.32	.69	1.16
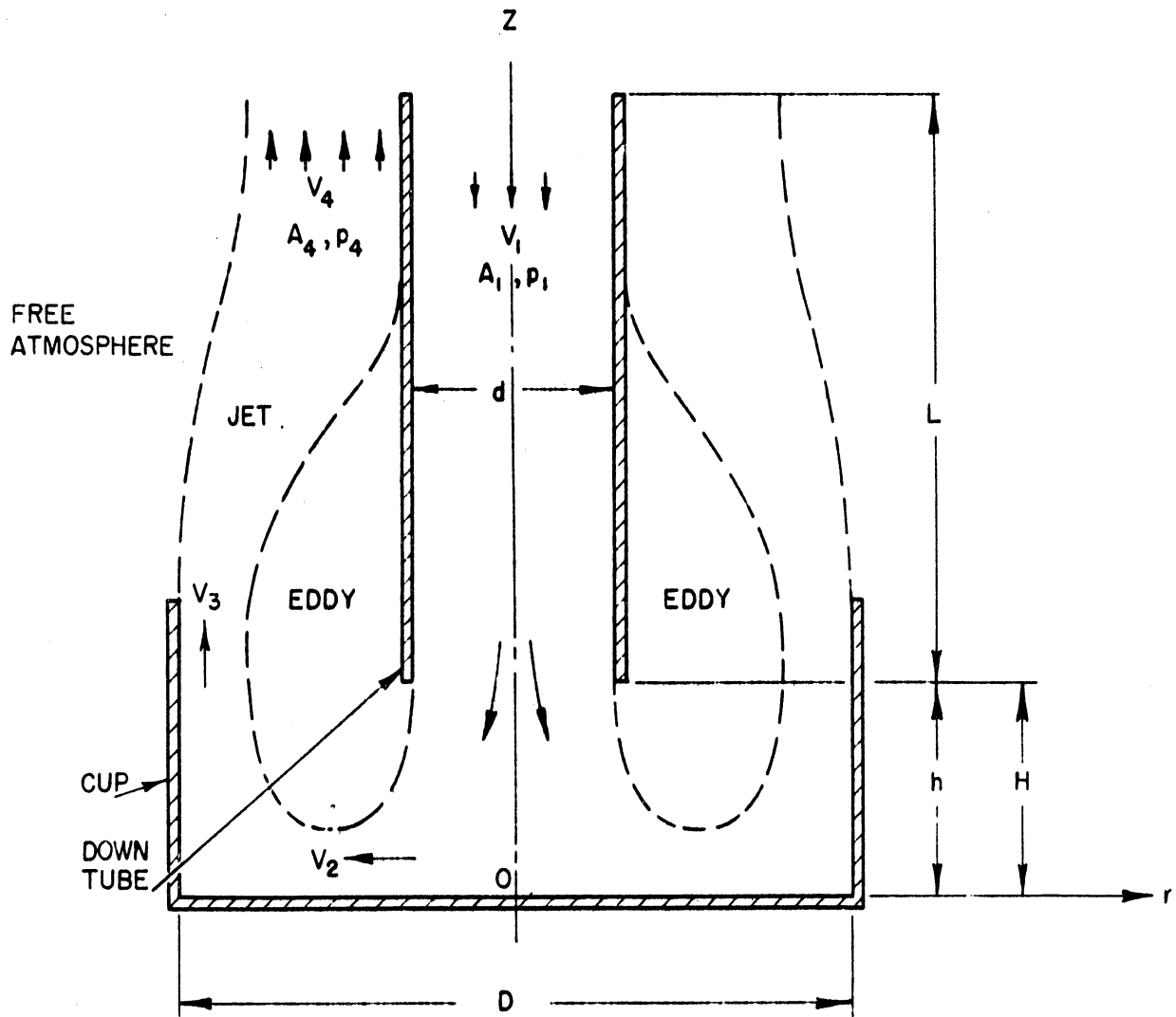
Fig. 10. The observed character of the air flow through the
cup region of the axially symmetric oil-spray test apparatus.

Symbols:

$$\Delta p = p_1 - p_4$$

$$R = \frac{V_1 d}{\nu}$$

$$\nu = \frac{\mu}{\rho}$$

μ = absolute viscosity of air

ρ = mass density of air

V = velocity

A = area

$\emptyset$ = pressure
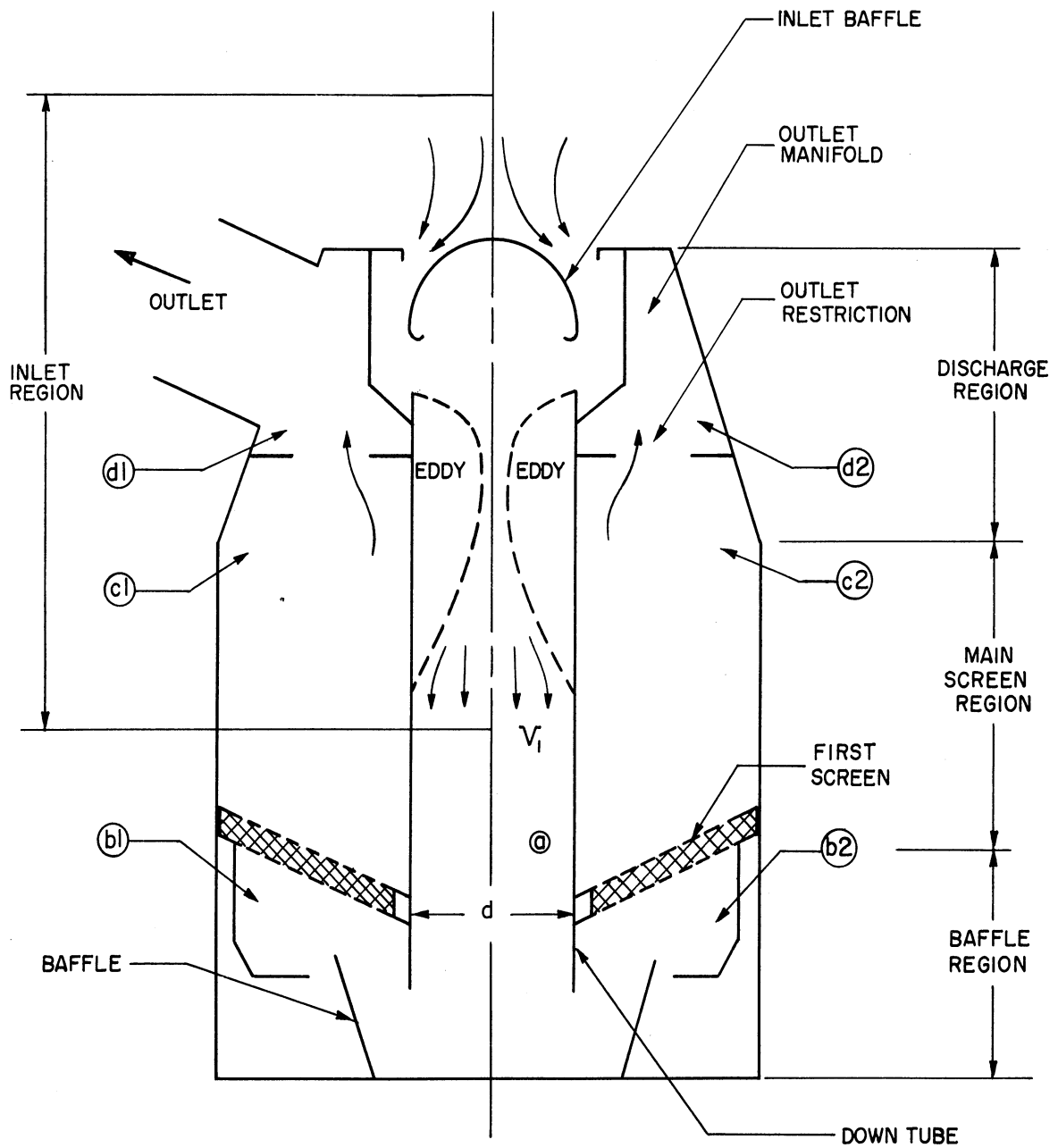
Fig. 11. Diametral section of the axially symmetric Donaldson (400 cfm) air cleaner. Points at which the pressure was measured are indicated by circled numbers.
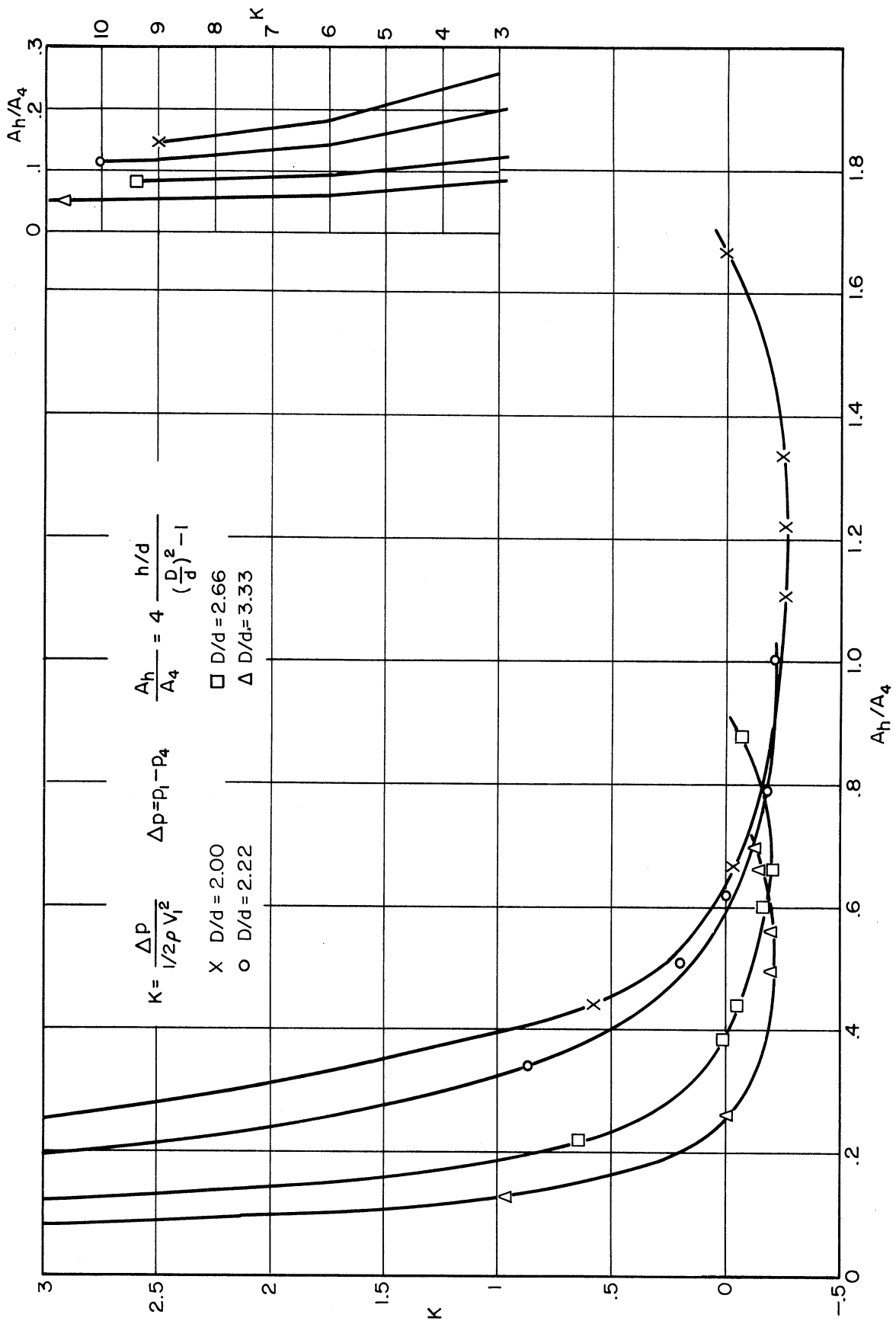
Fig. 12. Experimental values of the pressure drop in the test apparatus.
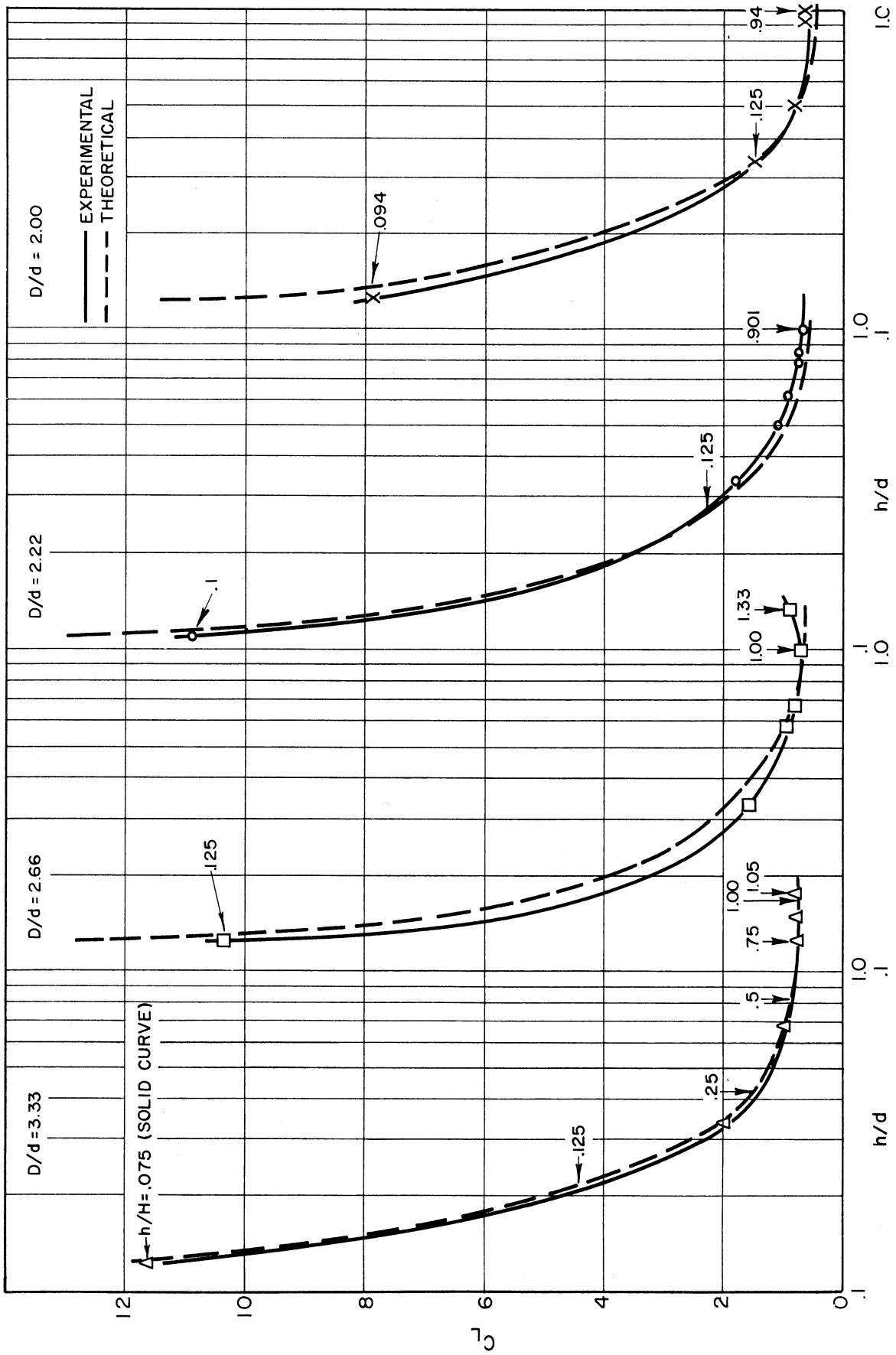
Fig. 13. Experimental and theoretical values of C_L in test apparatus.
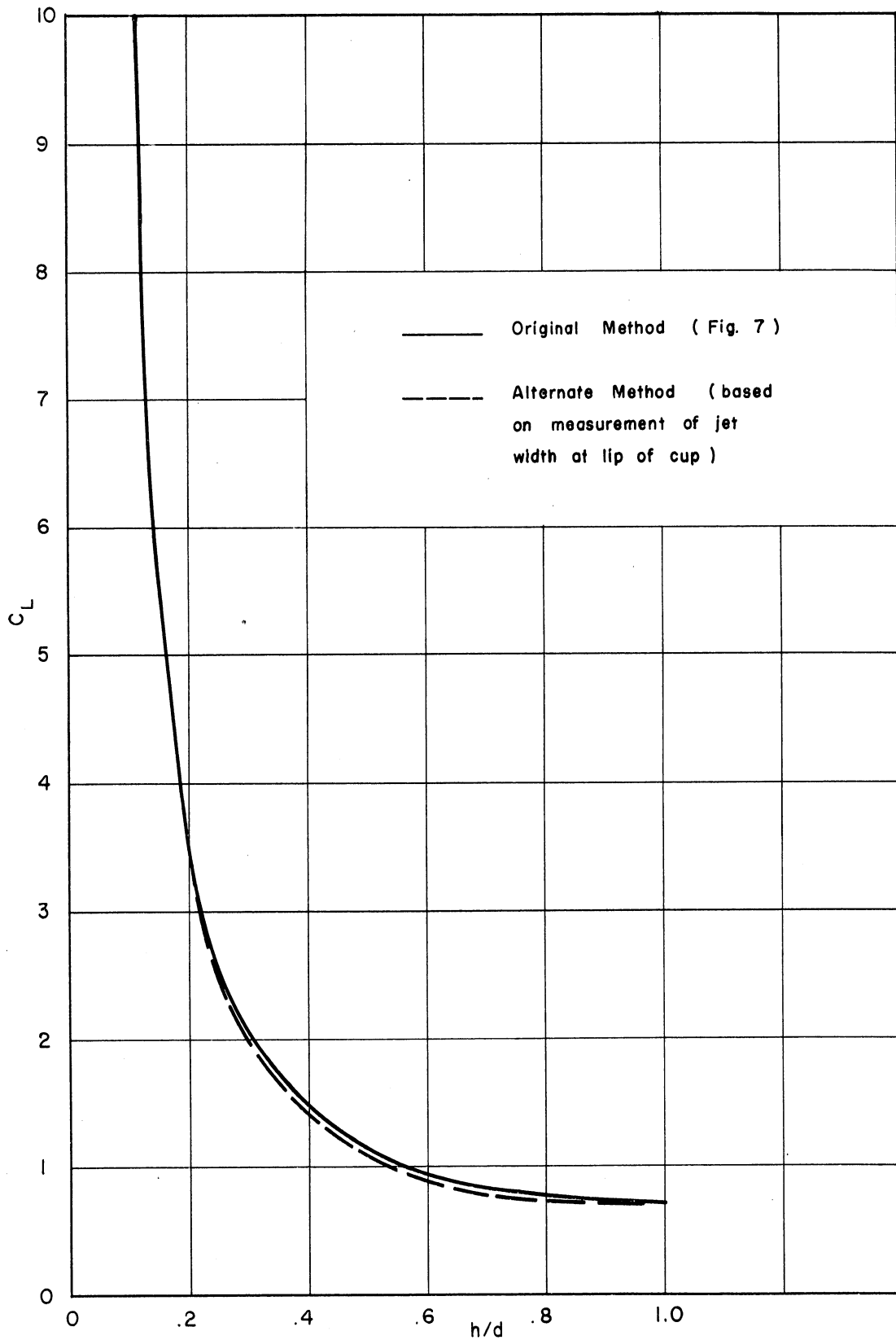
Fig. 14. Comparison of experimental values of C_L obtained by independent methods for $D/d = 2.22$.
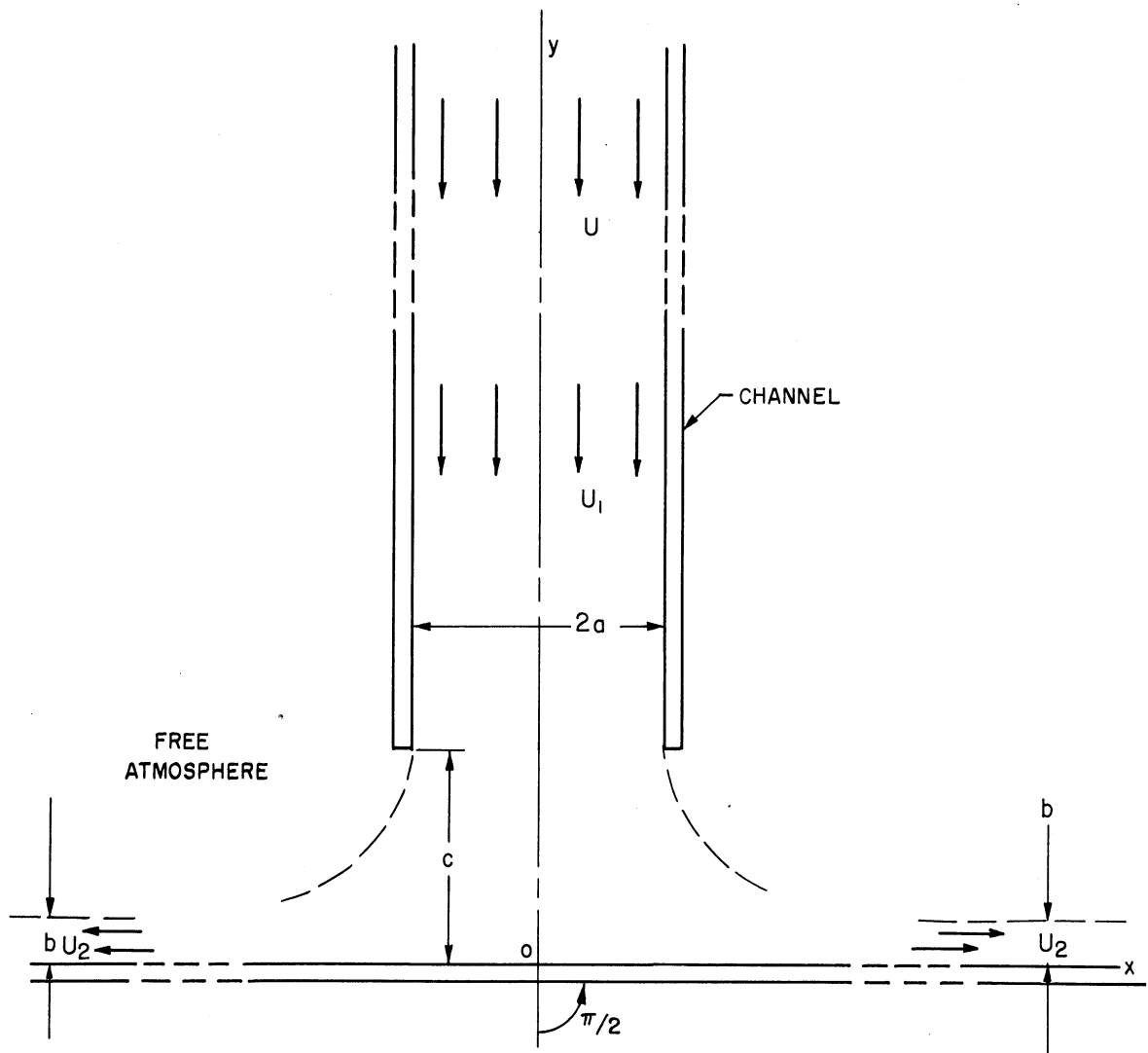
Fig. 15. The theoretical character of the flow of an incompressible, inviscid fluid in the case of the efflux from a two-dimensional channel against an infinite plane barrier perpendicular to the channel. U is the velocity for very large values of y and is assumed uniform across the channel. U_1 is the velocity a short distance above the channel outlet and is not uniform in general.
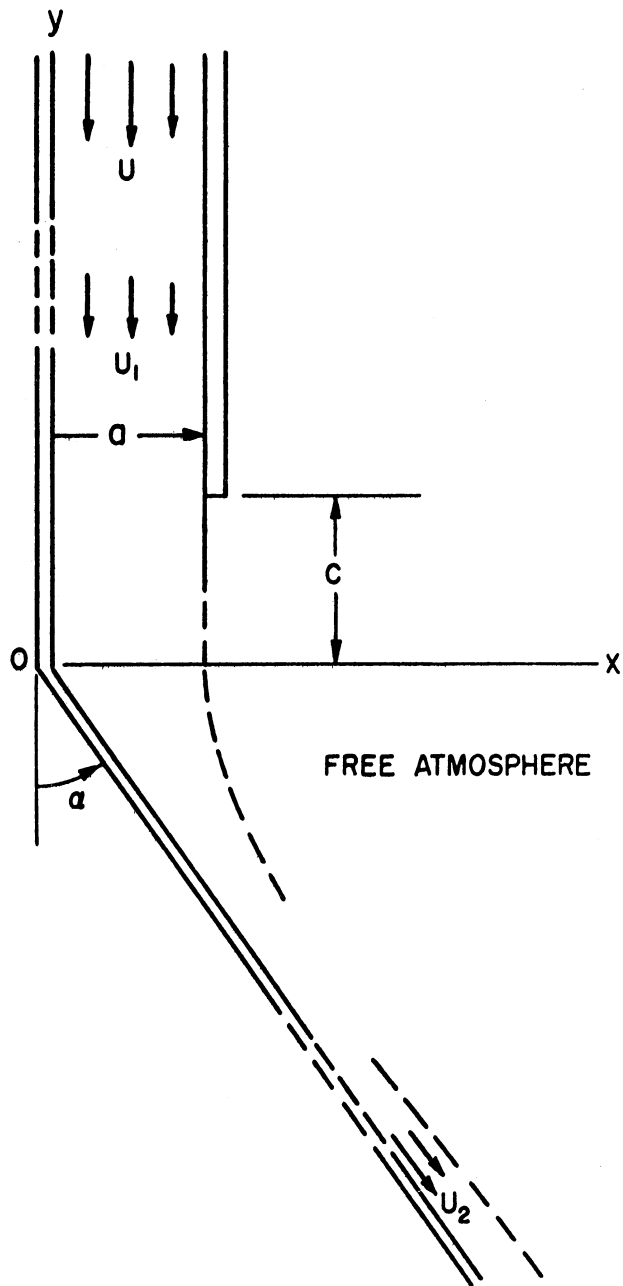
Fig. 16. The theoretical flow of an incompressible, inviscid
(ideal) fluid in the case of the efflux from a two-dimensional
channel against a semi-infinite plane barrier at an arbitrary
angle. With $\alpha = \pi/2$, this flow becomes identical with that
in the right- or left-hand half of Fig. 11.
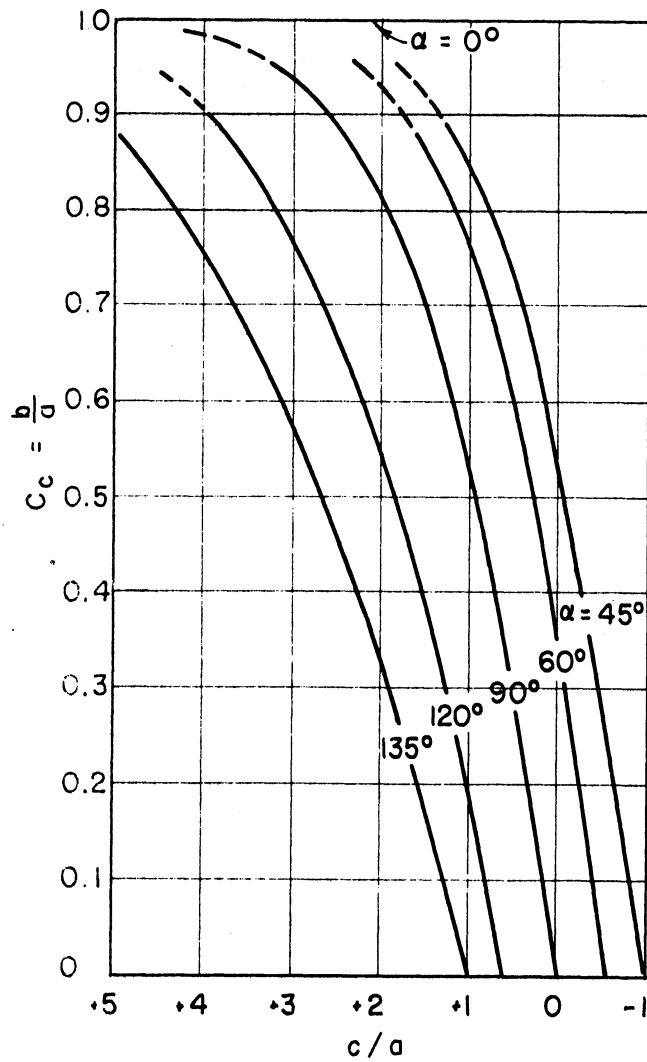
Fig. 17. Coefficient of contraction
for the problem of Fig. 16.
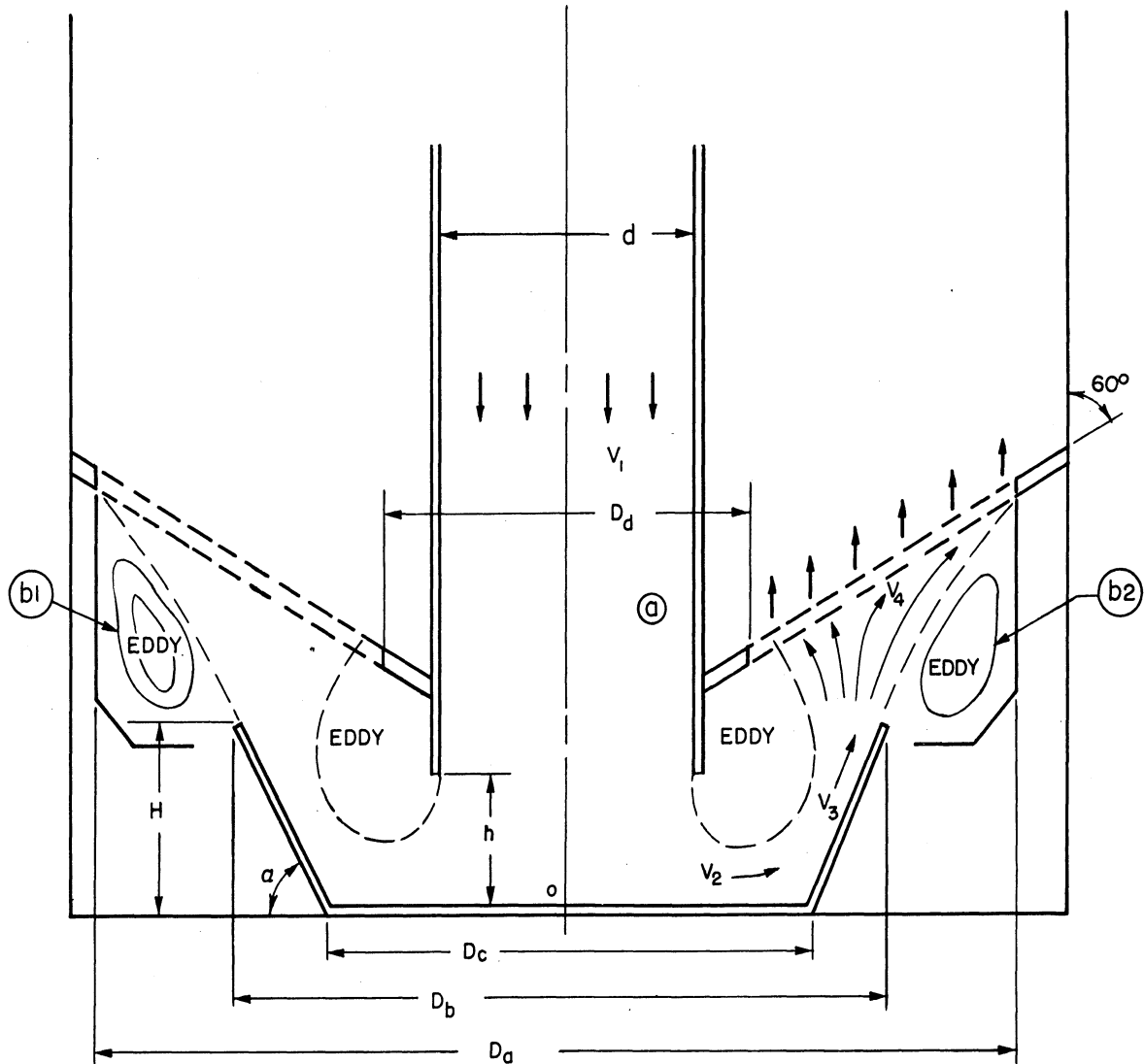
Fig. 18. The character of the actual flow of air through the baffle region of the axially symmetric Donaldson (410 cfm) air cleaner.

Note: Approximately, $d = 4.5"$, $h = 1.63"$, $H = 2.5"$, $D_a = 11.188"$, $D_b = 8.0"$, $D_c = 6"$, $D_d = 6.5"$, $\alpha = 68°$.
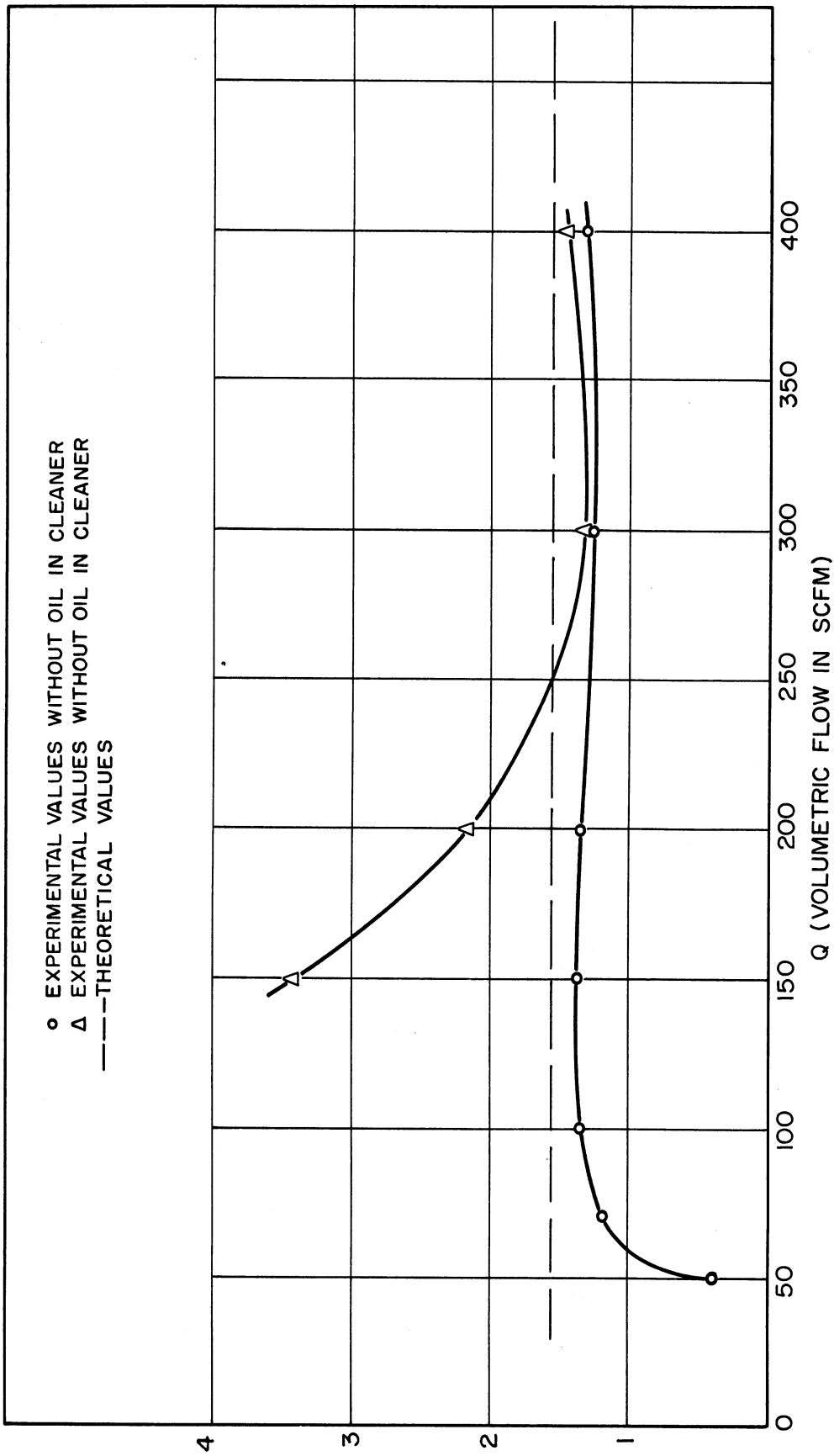
Fig. 19. The pressure drop in the baffle region of the Donaldson 410-cfm air cleaner.
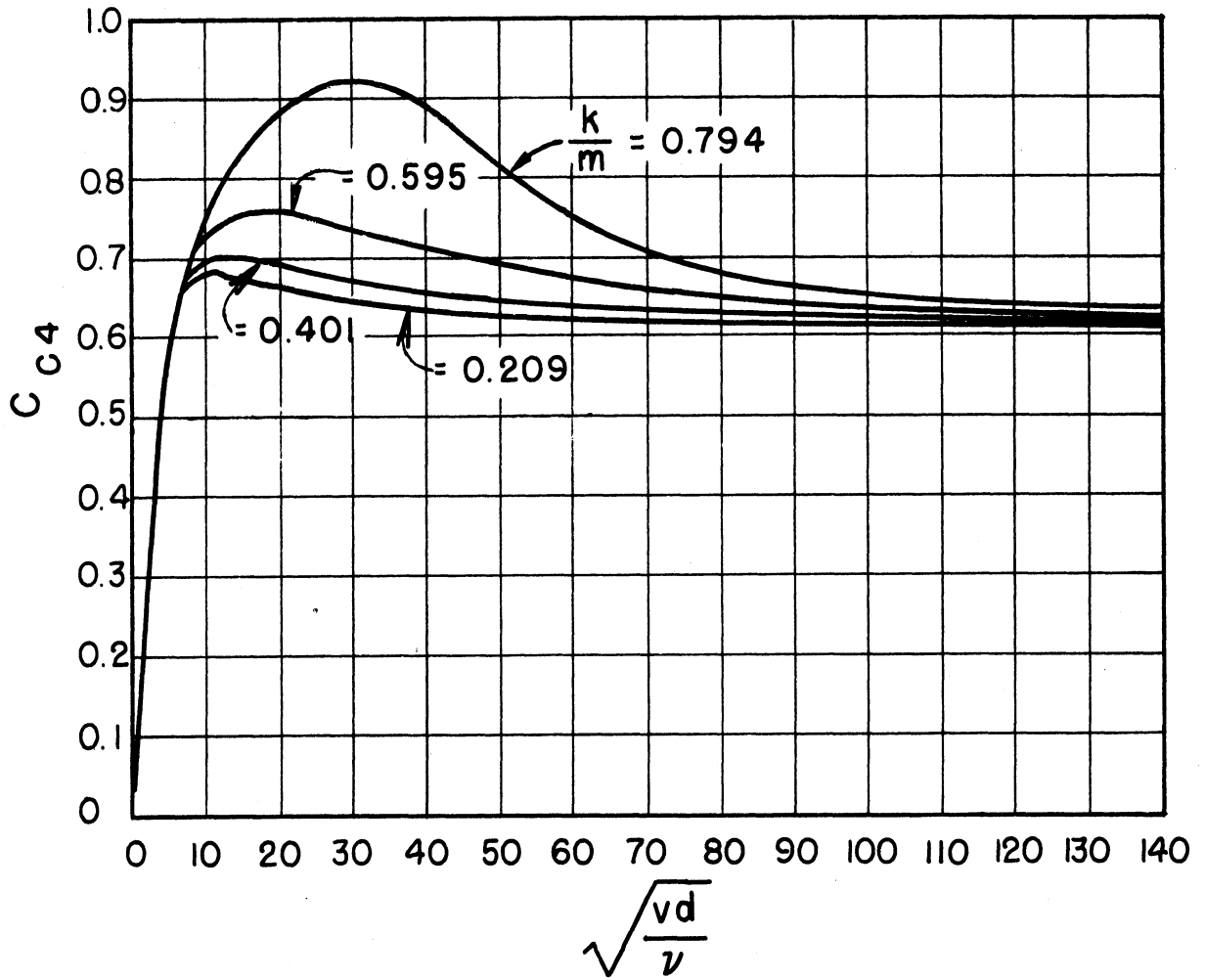
Fig. 20. Discharge coefficients for the plate orifice.
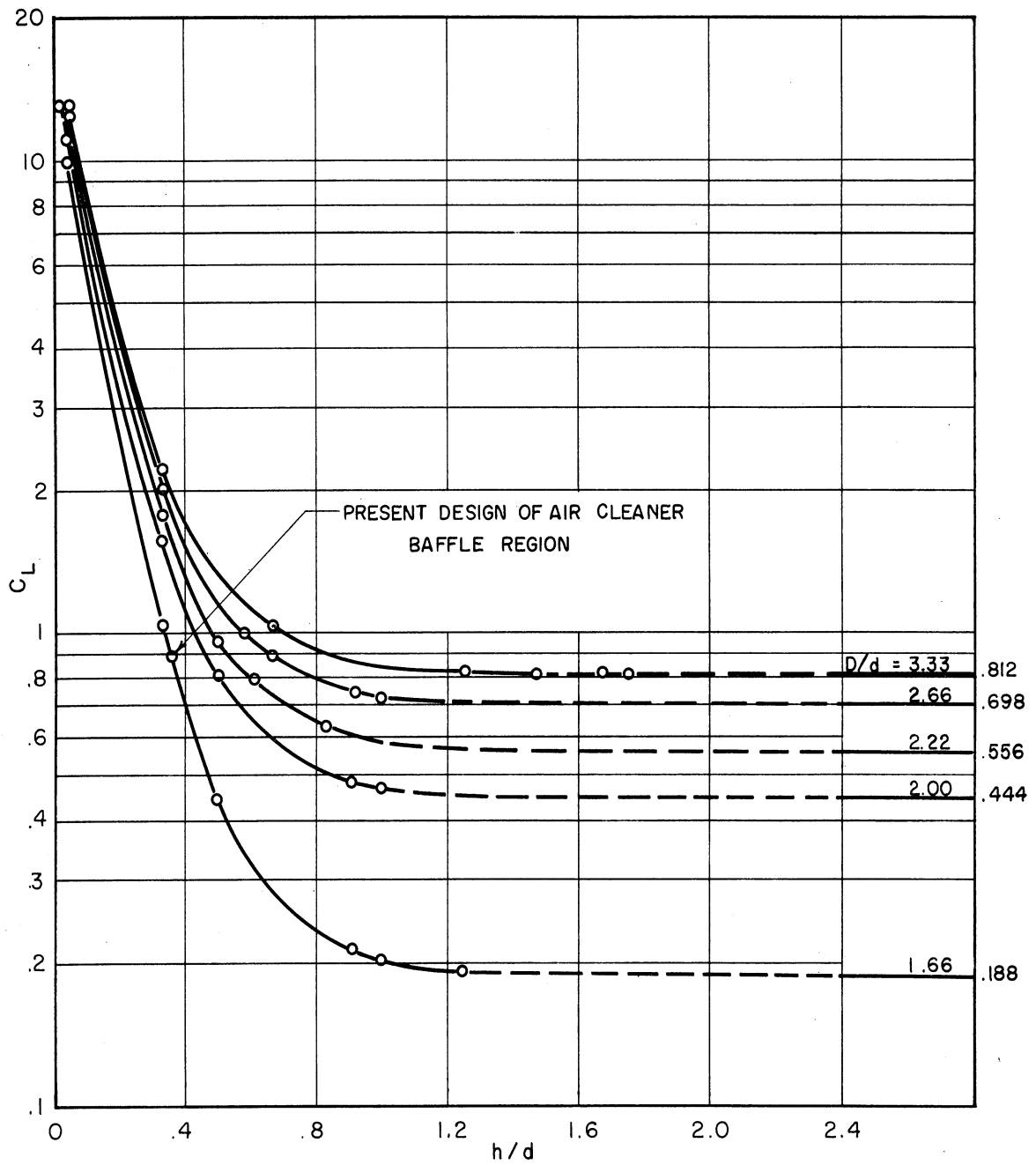
Fig. 21. Theoretical values of C_L for the baffle region of the test apparatus and the air cleaner.
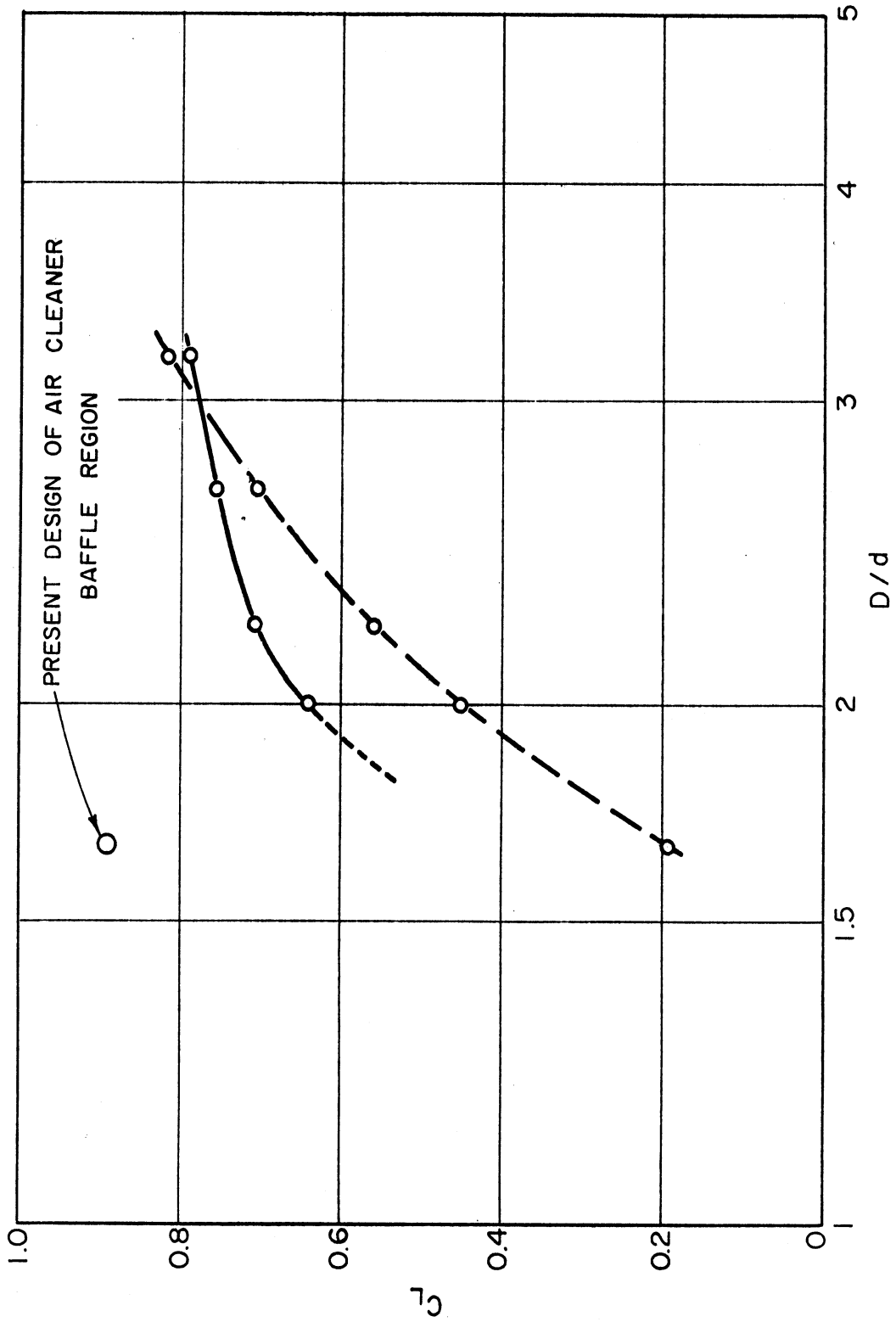
Fig. 22. Minimum values of C_L for the baffle region of the test apparatus and the air cleaner.
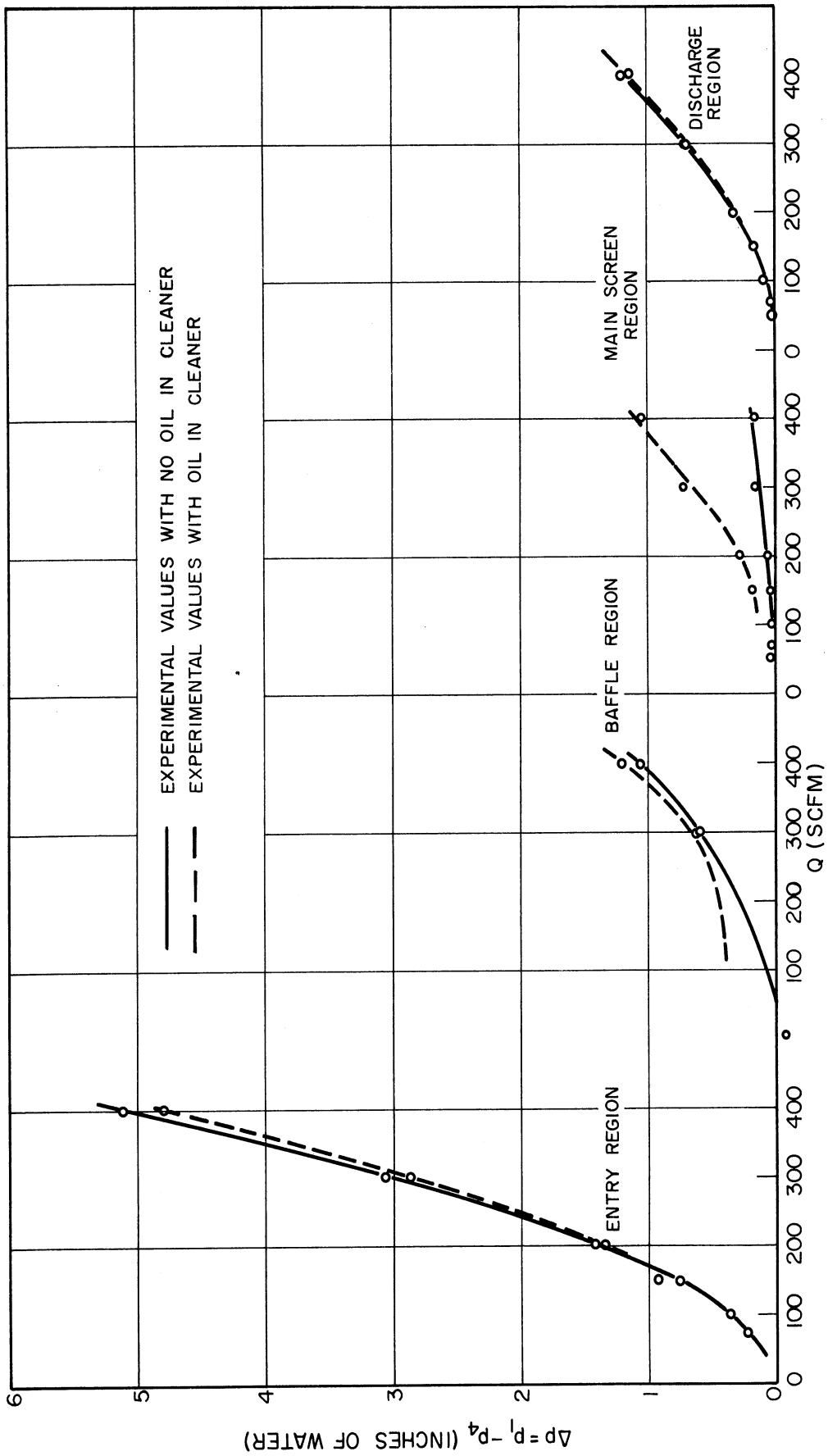
Fig. 23. Average pressure drops in various regions of the air cleaner.
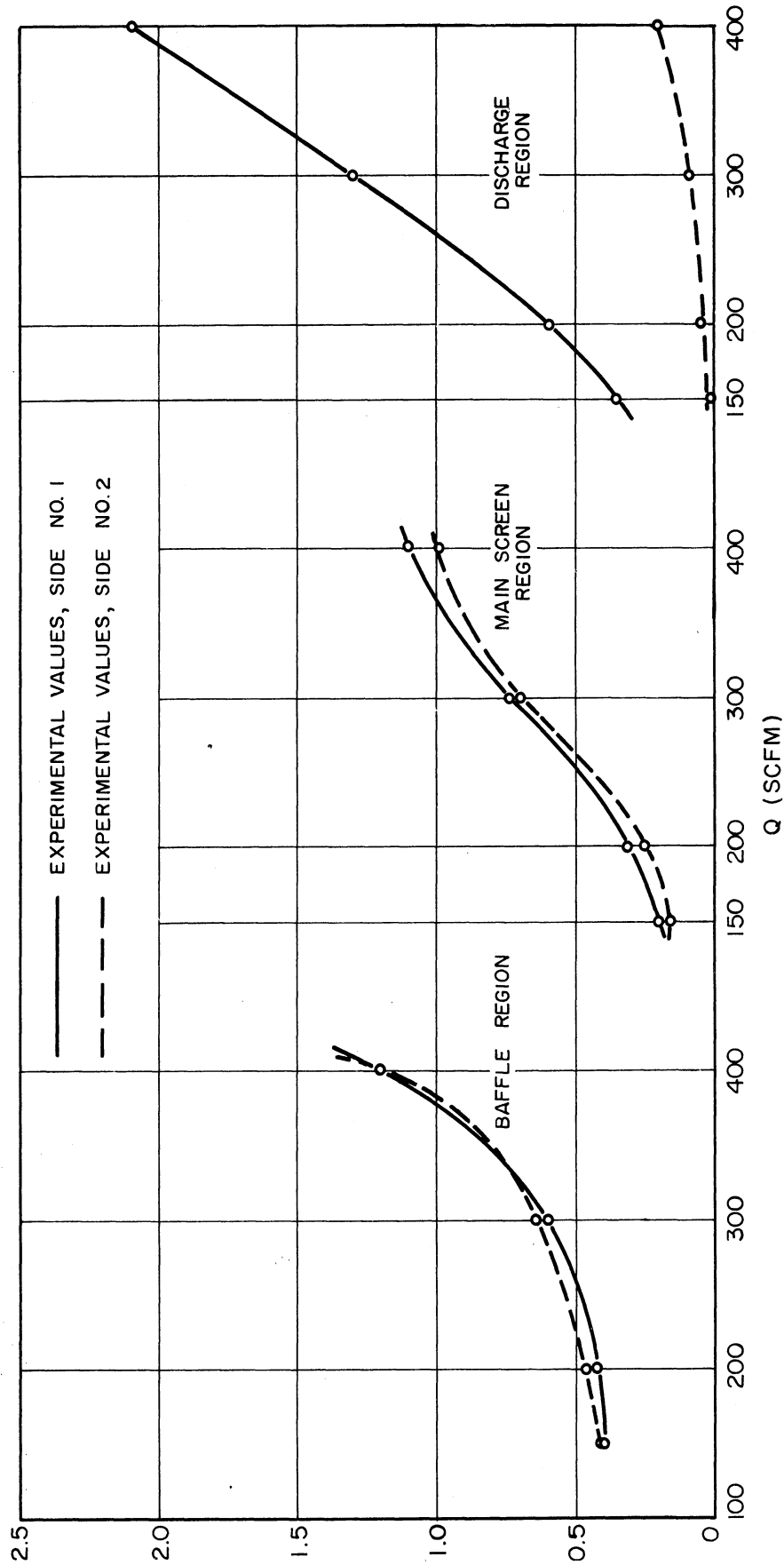
Fig. 24. Circumferential distribution of flow in the air cleaner as indicated by the pressure drop on the outlet side (No. 1) and the opposite side (No. 2) (with oil in cleaner).

APPENDIX B

(This appendix is photographically reproduced
and figure and page numbers are not continuous
with those in this final report.)

CHAPTER III

FLOW STREAMLINES IN AN AIR CLEANER;
EFFECTS OF GEOMETRY ON FLOW PATTERN

Introduction

Streamlines were photographed in a two-dimensional model of a Donaldson 410-cfm air cleaner placed in a water channel. The flow was made visible by means of powder on the free surface of the water. The geometry of the model could be varied.

Streamlines were also photographed for the flow of air through the three-dimensional cup-and-tube test apparatus consisting of a vertical downtube discharging into an upturned cup having a vertical side wall. In this instance, the flow was observed by means of a smoke stream.

The effects of geometry on the flow pattern are most conveniently studied by means of a free-surface flow of water through a two-dimensional model. The validity of the results for qualitative conclusions is discussed and may be seen by a comparison of Figs. 34 and 38, which have the same geometry and represent, respectively, the flow of water through a two-dimensional model and the flow of air through the three-dimensional test apparatus.

The Air Cleaner

It was decided to study first the flow through configurations similar to that of the Donaldson 410-cfm air cleaner. Figure 25 shows one half of a diametral section in the plane containing the discharge opening of the cleaner. For convenience in discussion, Fig. 25 divides the flow path into sections designated as the entry, baffle, main screen, and discharge regions.

Description of the Two-Dimensional Model

Figure 26 is a plan view of the type of model used in the water channel. The geometry could be varied, and Fig. 26 shows that of the Donaldson cleaner. A maximum of two screens was used in the main screen section. In actuality, this region is entirely filled with screen material (Fig. 25). However, the use of one or two screens at particular cross sections was successful in suggesting the principal effects which the screens may have on the flow through them. Due to the use of a water channel, it was necessary to divert the discharge flow through an angle of 180°; therefore, the streamlines downstream from the outlet restriction are not representative of conditions in the air cleaner.

The model was constructed of 1/32-inch-thick brass strips, the edges of which are seen in Fig. 26. As can be seen by comparing Fig. 26 to Fig. 27 or 28, the brass strips appear to be much thicker than 1/32 inch in the photographs, due primarily to parallax and to the refraction of light by the meniscus on the water surface adjacent to the brass strips.

Since it is a two-dimensional representation of a three-dimensional cleaner, the model cannot have true geometrical similarity. However, the latter condition was realized approximately by making the model to a scale of one-third of the actual size of the cleaner as it appears in a diametrical cross section. The lack of true geometric similarity results primarily in the flows at large radii in the air cleaner having relatively lower velocities than those at corresponding points of the model.

When geometrical similarity exists, the model should be tested at water flow rates giving the same range of Reynolds' number as that of the air flow rates encountered in operation of the full-scale air cleaner. Consequently, a direct comparison of the Reynolds' numbers of the model and cleaner has no significance in this case. However, the flow pattern in the baffle section may be expected to vary only slightly with the Reynolds' number. In the screen sections of both the model and cleaner, the velocities are smaller and the flow path is not as definitely dictated by the boundaries. Here the Reynolds' number is a factor and, furthermore, the screens themselves were not reproduced to scale. In this region only limited conclusions may be drawn from the photographs. Nevertheless, the pictures are useful in determining the character of flow entering the screen section and the influence which a change in baffle geometry would have on an existing screen flow.

The use of a free-surface water flow introduces surface tension as a factor not present in the air cleaner. However, its effect may be assumed negligible for present purposes.

Flow in the Entry Region

The flow past the entry baffle and through the central down-tube of the cleaner may be seen along the left hand edge of Fig. 34. In the upper part of the tube, an elongated toroidal eddy near the wall restricts the axial flow. Farther down, the velocity becomes fairly uniform all across the tube. Some of the pressure drop due to the higher velocity of the stream in the eddy section will be regained in the region of uniform flow. However, the net result should be an appreciable loss, due to the diffusion in the expanding flow from the eddy to the point where the velocity becomes uniform across the tube.

This restriction of the flow can be greatly reduced by the addition of a deflector vane to divert a portion of the flow through the region now occupied by the eddy. Preferably, the vane should be designed as a part of a general redesign of the entry region and the hemispherical entry baffle. But if other considerations make it undesirable to change the latter, a vane can be designed as an addition to the present cleaner. This point is discussed more fully in Chapter II.

The General Character of the Flow Through the Baffle and Screen Regions

The photographs of flow through the model, Figs. 27 through 36, will be surveyed briefly before turning attention to details of the baffle and screen regions.

1. Absence of baffle (main stream located near inner wall of main screen section—Figures 27 and 28).

In the absence of a baffle, the flow adheres to the outer boundaries in the baffle region. It must ultimately deflect inwardly (to the left) in order to leave the screen region. The outer clamping bracket of the first screen determines the location of this deflection (Fig. 27). The stream in the screen region is narrow. The addition of the first screen (Fig. 28) has little effect on the stream, but does introduce an intense and stable eddy below the screen and adjacent to the down-tube.

2. Slanted baffle (main stream located near outer wall of the main screen section—Figs. 29, 30, 31, and 32).

With a slanted baffle (Fig. 29), the stream follows the outer boundaries of both the baffle and screen sections. The addition of the first screen (Fig. 30) does not alter the path of the flow in the screen region, although the stream is wider and of more uniform velocity over its cross section. ,The flow is quite uniformly distributed across the first screen.

When the first screen becomes plugged near its inner edge (Fig. 31), the stream in the screen region remains wide and uniform. If the screen is plugged near its outer edge (Fig. 32), the stream narrows and flows through the center of the screen section with an eddy region on either side.

3. Slanted baffle (main stream located near inner wall of screen section—Fig. 33).

While the foregoing indicates the outward influence of the slanted baffle on the flow in the screen section, plugging downstream from the first screen may override the action of the baffle. A second screen (Fig. 33) plugged near its outer edge can permanently deflect the stream inwardly even though the slanted baffle is used.

4. Vertical and horizontal baffles (main stream located near inner wall of main screen section—Figs. 34, 35, and 36).

When the baffle is vertical (Fig. 34), the stream is narrow and hugs the outer periphery of the baffle section and the inner periphery of the screen region. The addition of the screen (Fig. 35) does not broaden the stream, which approaches the screen at right angles and remains narrow in the screen region. A comparison of Figs. 28 and 35 indicates that the insertion of a solid boundary (vertical baffle) at the edge of the stream has no effect on the flow path.

A horizontal baffle (Fig. 36) serves to broaden the flow in the screen section, the stream remaining adjacent to the inner boundary.

Control of Flow Pattern in the Baffle and Screen Sections

It is clear that within wide limits the flow in the baffle and screen regions can be made to assume a prescribed pattern. The control can be accomplished by proper design of the baffle region and of the orientation of the first screen, and will be effective as long as the screen region remains unplugged in areas traversed by the main stream. Some specific examples follow.

LOCATION OF MAIN STREAM IN SCREEN REGION

Figures 30 and 36 show fairly wide and uniform streams in the screen region near the outer and inner boundaries, respectively. A different design of the baffle and position of the first screen should permit the flow to approach, to the extent desired, a uniform distribution across the entire screen section. Presumably, the most desirable flow pattern in the screen section is partially determined by any return oil flow which is intended to occur. It is clear that the eddy region bounding the main stream may be located at either the inner or the outer boundary as desired. New designs can be worked out through the use of the channel.

FLOW ALONG THE BAFFLE

Figures 29 through 36 indicate that a curved baffle would direct a more effective jet at the first screen. Such a baffle may also reduce the pressure loss in this region and, if desirable, assist in maintaining the eddy under the outer part of the first screen.

OUTER EDDY IN THE BAFFLE REGION

Figures 30, 31, 32, and 33 have the baffle configuration of the Donaldson cleaner. The outer (right hand) portion of the space immediately below the first screen is occupied by an eddy rotating clockwise. In Fig. 32 where the outer part of the first screen was plugged, this eddy was very stable over a range of flow rates and entirely filled the outer portion of the space below the screen. Under the conditions of Figs. 30, 31, and 33, the eddy was erratic and at some flow rates did not extend down to the partition immediately below it. At such times, the fluid just above this partition was either oscillating or rotating slowly in a counter-clockwise sense.

PLUGGING OF THE SCREENS

Unavoidable loading of portions of the screens during operation may cause the flow in the main screen region to deviate significantly from any desired pattern achieved at the outset. If this condition unduly curtails the period of effective operation of the cleaner, the cleaner should be redesigned so that unavoidable loading is more uniformly distributed throughout the screen region. A need for more uniform flow in the screen of the discharge region is shown in Chapter II. Some remedies are suggested there.

Air Flow Streamlines in the Cup-and-Tube Test Apparatus

The air flow in this apparatus was studied by introducing smoke at the bottom of the upturned cup. Specifically, smoke was inserted at a point where the air had left the down-tube and was flowing radially outward parallel to the bottom of the cup. The apparatus and the air flow were symmetrical about the vertical axis of the down-tube. The flow boundaries formed by the down-tube and cup are indistinct in the photographs obtained. Consequently, a drawing (Fig. 37) is included which shows the portion of the apparatus in which the flow was photographed.

Figure 38 is a photograph of the flow through the cup and upward along the outer surface of the down-tube. The outlet of the smoke supply tube can be seen at the bottom of the cup. The approximately elliptical region just above the smoke tube outlet was the location of a stable eddy which appears as a dark region since it contained very little smoke. At greater air flows this eddy became elongated and extended higher up the outer surface of the down-tube. As in the analogous two-dimensional case (Fig. 34), Fig. 38 clearly shows that, after passing the stationary eddy, the jet is diverted radially inward and flows along the surface of the down-tube. Higher up the tube, the air stream broadens gradually.

The dark region above the cup and to the left of the main stream is the location of a large, slowly rotating eddy similar to those already seen in the two-dimensional cases. Figures 39 and 40 show the beginning of a small eddy of a type generated at intervals on the boundary between the jet and the large boundary eddy. Such eddies were then drawn upward by the stream, as indicated by Fig. 38, where an eddy can be seen at the top of the photograph. This unsteady condition at the edge of the stream was predominant at lower flows under which circumstances fluctuations in the total flow rate were observed. A similar behavior was noted occasionally in the water channel. In the air cleaner, it is expected that the distributed screens will suppress this effect.

Flow Around the Lower End of the Down-Tube

The stationary eddy observed above the smoke tube outlet (Fig. 38) was decidedly present in the corresponding part of the two-dimensional model where it appeared just below the inner (left hand) end of the first screen. However, it is not clearly shown in the photographs (Figs. 29 through 36) because in some instances (Fig. 34, especially) the film exposure was too short

for this purpose, and in other cases the meniscus and parallax caused an apparent broadening of the nearby boundary and obscured part of the eddy.

By placing a rounded obstruction on the inner surface of the downtube just above its lower end, the stationary eddy was nearly eliminated in the two-dimensional model. This obstruction is indicated by a dotted line in Fig. 26. The elimination of this eddy should assist in obtaining a wide uniform stream in the screen region and may reduce the pressure loss somewhat. Such a change produces a more uniform flow in the baffle region, but reduces the velocity of the fluid leaving the cup, especially at the upper end of the slanted baffle.

Pressure Loss in the Air Cleaner

Suggestions have been made in foregoing sections for reducing the pressure loss in the air cleaner, particularly at the upper and lower ends of the down-tube. However, such reductions may be negligible compared to the necessary loss in the screen or other regions. In order to investigate this phase of the problem, measurements were made of the pressure loss in each of the regions of the cleaner. This work is described in Chapter II and, together with the results of the present chapter, leads to several conclusions regarding air-cleaner design.

Summary and Conclusions

While some important conclusions have been reached, it may be desirable to obtain additional flow pictures. The present method for photographing the flow was worked out only recently, and the experience gained has suggested improvements in the technique which should result in more readily interpreted photographs.

The flow pictures indicate that the air flow in the cleaner can be studied in the water channel and can be controlled through the design geometry. It appears that the flow in the screen region is nonuniform and that a curved baffle and an obstruction of the bottom of the down-tube may improve this condition. A vane below the entry baffle should reduce the pressure drop considerably. A full appraisal of these changes requires measurements of the pressure drop in the various regions of the air cleaner. Such data are analyzed in the earlier chapter on pressure drop and pressure loss in the air cleaner.
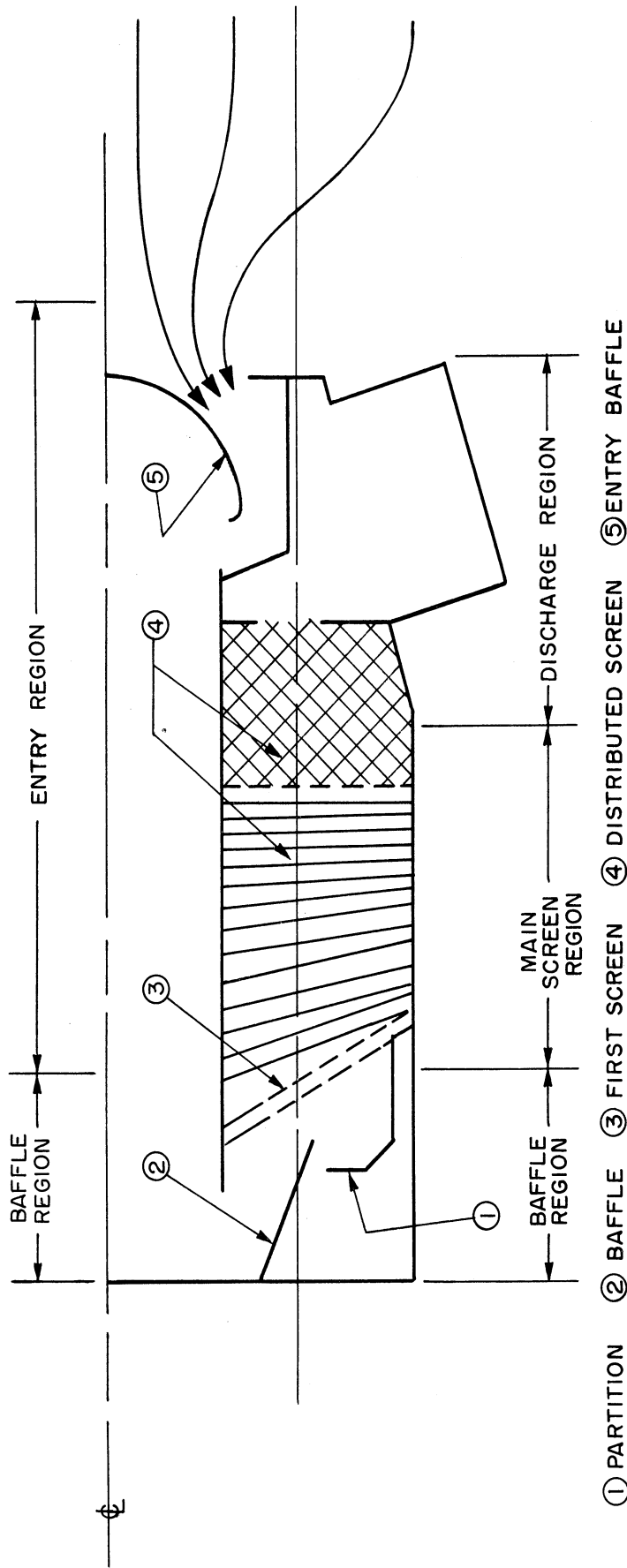
Fig. 25. Half section through Donaldson 410-cfm air cleaner.

① PARTITION   ② BAFFLE   ③ FIRST SCREEN   ④ DISTRIBUTED SCREEN   ⑤ ENTRY BAFFLE
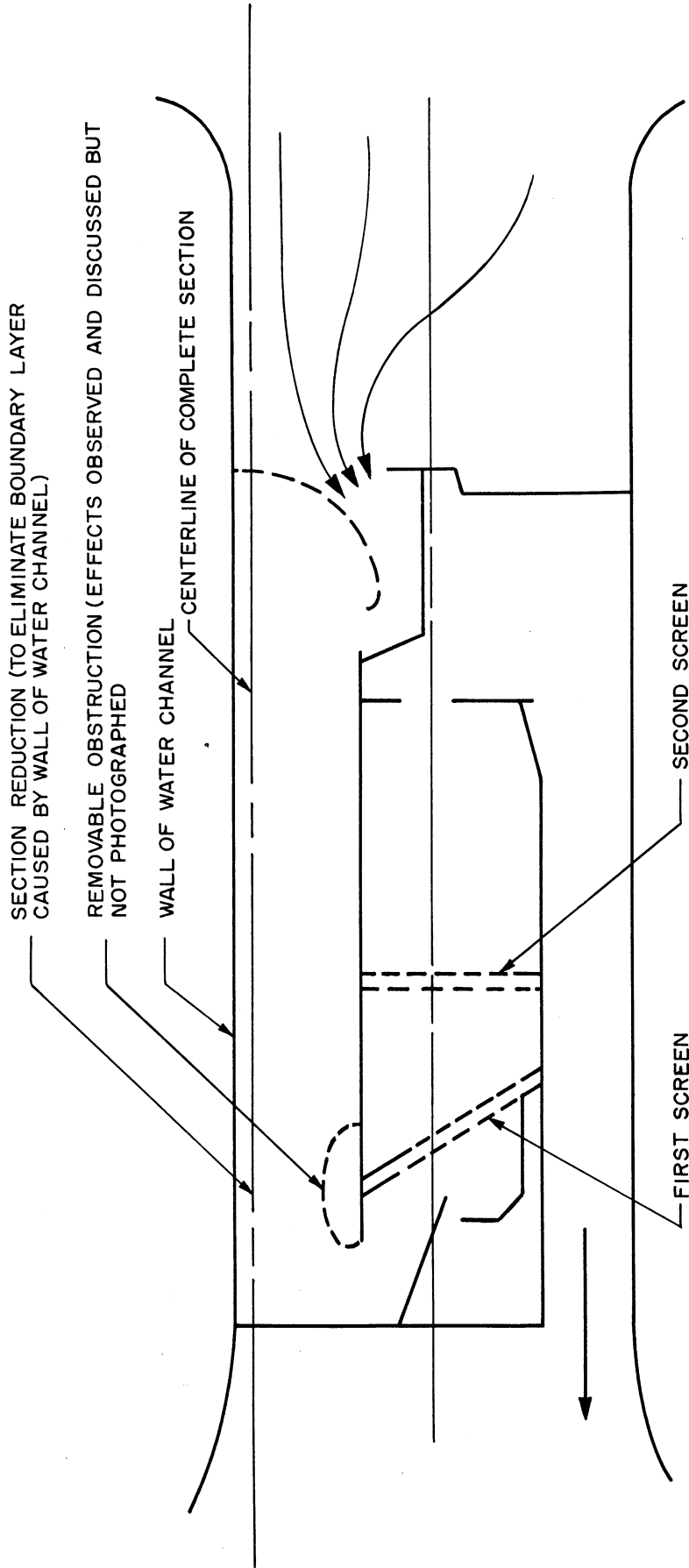
Fig. 26. Plan view of two-dimensional model of Donaldson 410-cfm air cleaner, representing one half of a diametral section of the air cleaner.

Note: See Fig. 1 for other names of components. Dashed lines indicate components removable in the model. The baffle and partition were removable in a second similar model.
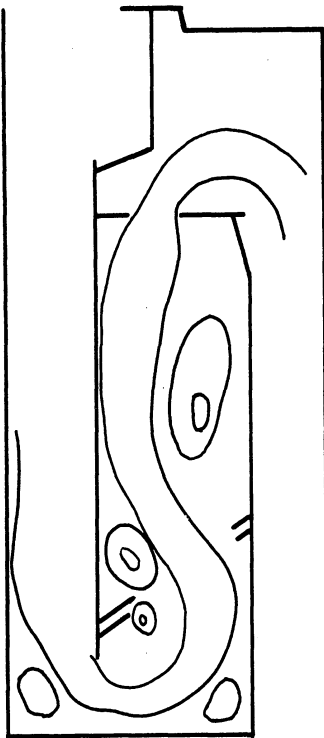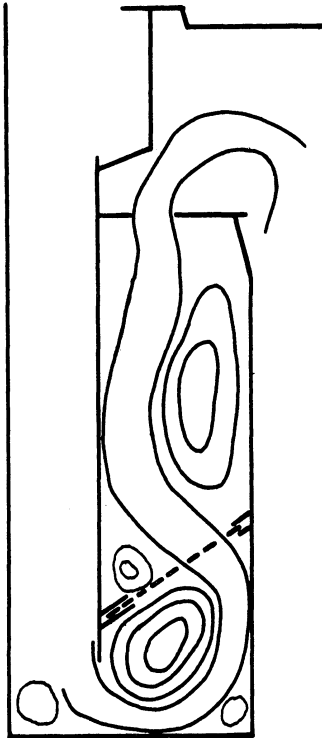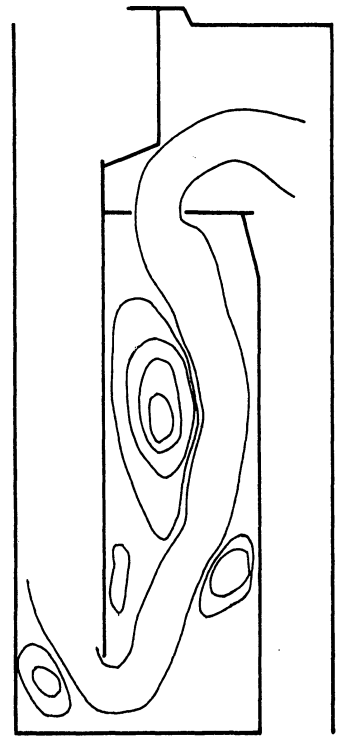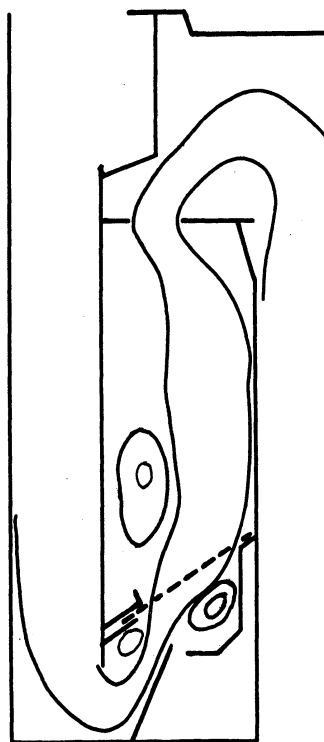
Fig. 27.

Fig. 28.

Fig. 29.

Fig. 30.
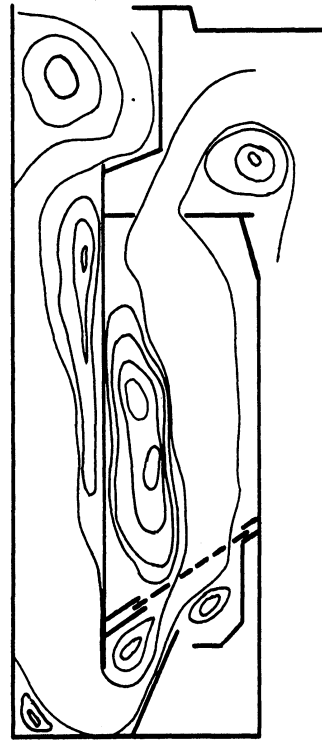
Fig. 31.
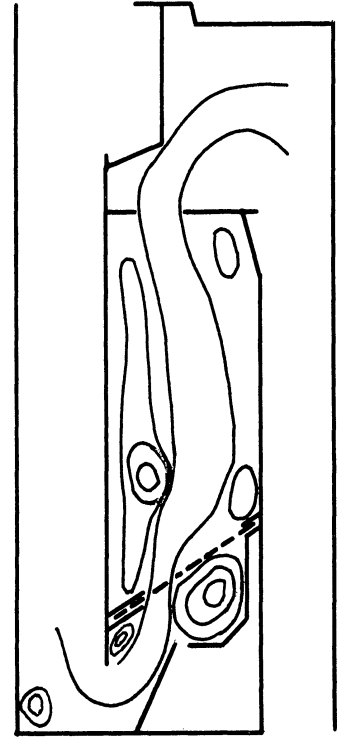
Fig. 32.
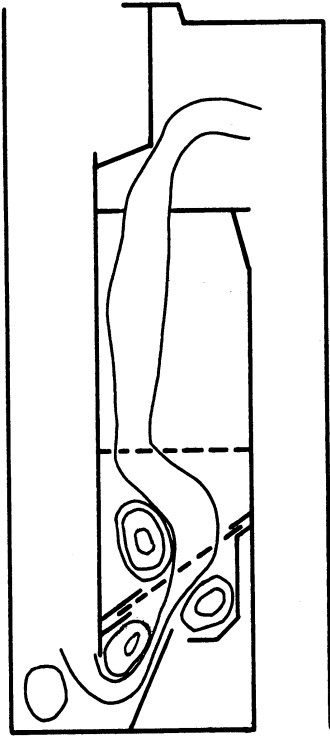
Fig. 33.
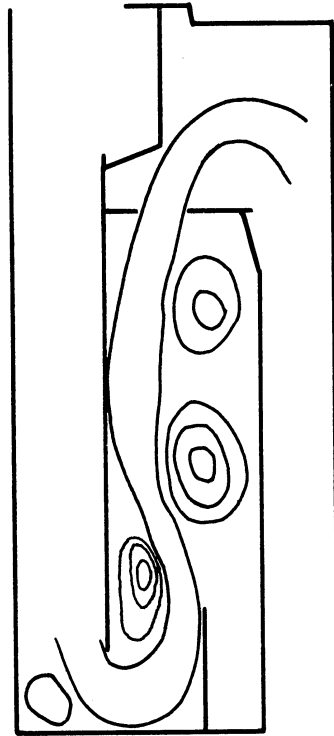
Fig. 34.
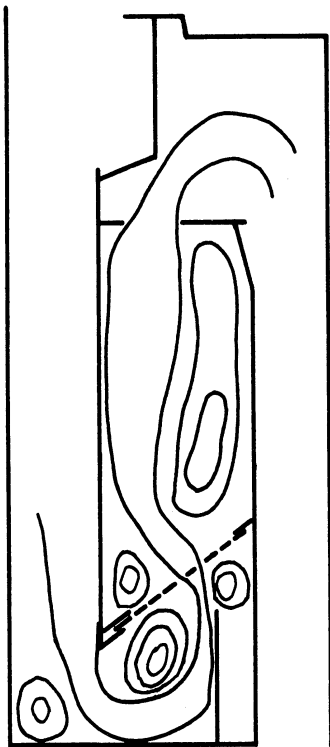
Fig. 35.
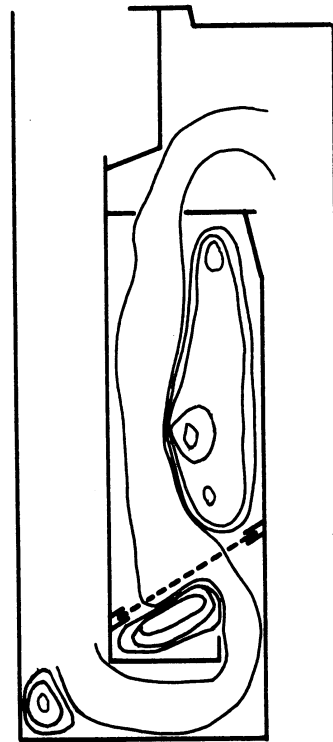
Fig. 36.

Fig. 38. Flow pattern.
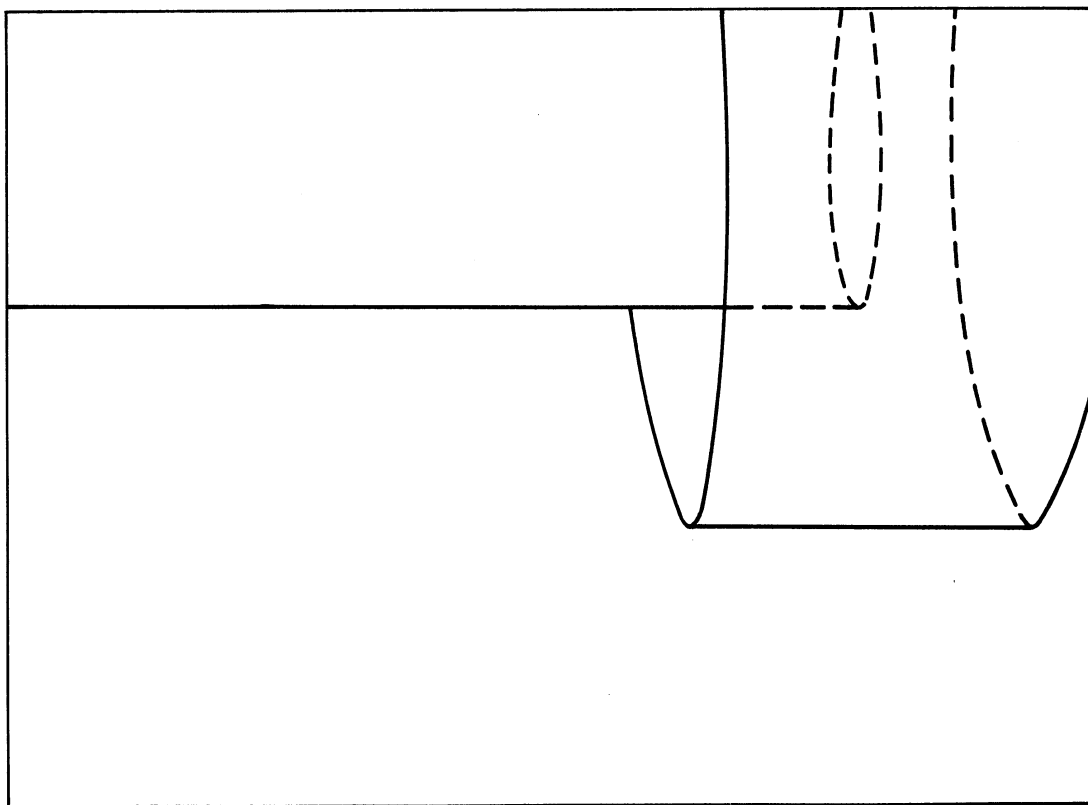
Fig. 37. Flow pattern.

Fig. 40. Flow pattern.
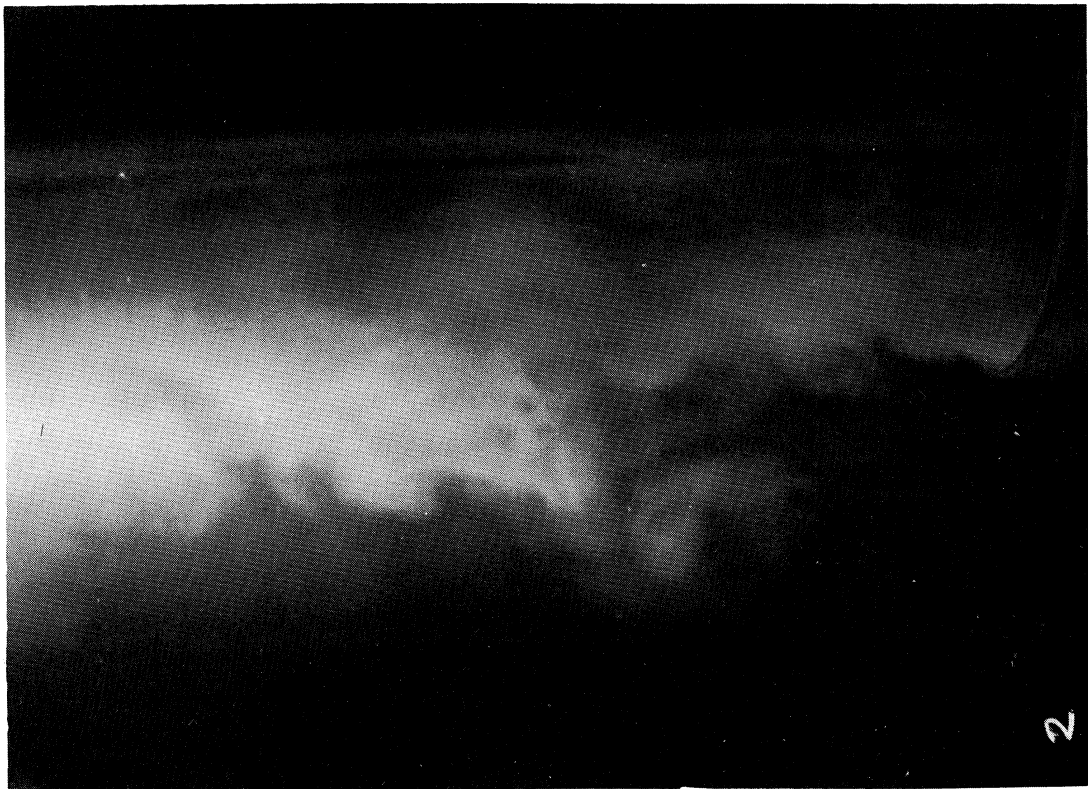
Fig. 39. Flow pattern.

APPENDIX C

Interim Technical Report No. 6

THE COLLECTION OF SALT DUST ON DRY WIRES

Seymour Calvert

The earlier work on dust collection efficiency of fibrous packing showed that the collection efficiency of a single fiber was not sufficient to define the efficiency of a group of fibers. A key factor is the amount of mixing, or redistribution of dust in the airstream, occurring after the air passes a fiber and moves toward the fibers downstream from it. This is discussed and some experimental data compared to predictions based on the extremes of no mixing and of complete mixing after each wire. Additional information was desired, however, and an experimental study was initiated.

A controlled grouping of wires was devised to give well-defined arrangements, varying wire spacing (in both directions), wire diameter, air velocity, and particle size. Spray-dried salt was chosen as the test dust, and the amount collected was determined by washing the salt off the collector wires. It was hoped that the common assumption would hold; i.e., that any particle striking a wire would stick to it. Presumably this would mean that dry wires would behave the same as wetted wires.

This proved to be wrong. After several runs it became apparent that collection efficiency was much lower than predicted. A long period of checking and rechecking all aspects of the experiment disclosed no experimental error. The data appear to be quite valid and a significant fact was established although the original purpose of the experiment could not be fulfilled during the limited experimental time.

Experiments on the collection of 0- to 5-micron salt dust on 0.003-inch-diameter parallel wires and 0.011-inch-diameter wire screen (14 mesh) indicate that collection efficiency is about one-half of that predicted. The effects of changing wire spacing in the direction of the air flow are discernible but minor.

EXPERIMENTAL METHOD

The experimental apparatus consisted of the following components which are illustrated in Fig. 1.

Sampler

Removable Sleeve

Collection Grids

Test Section

Spray Drier

Air Drier
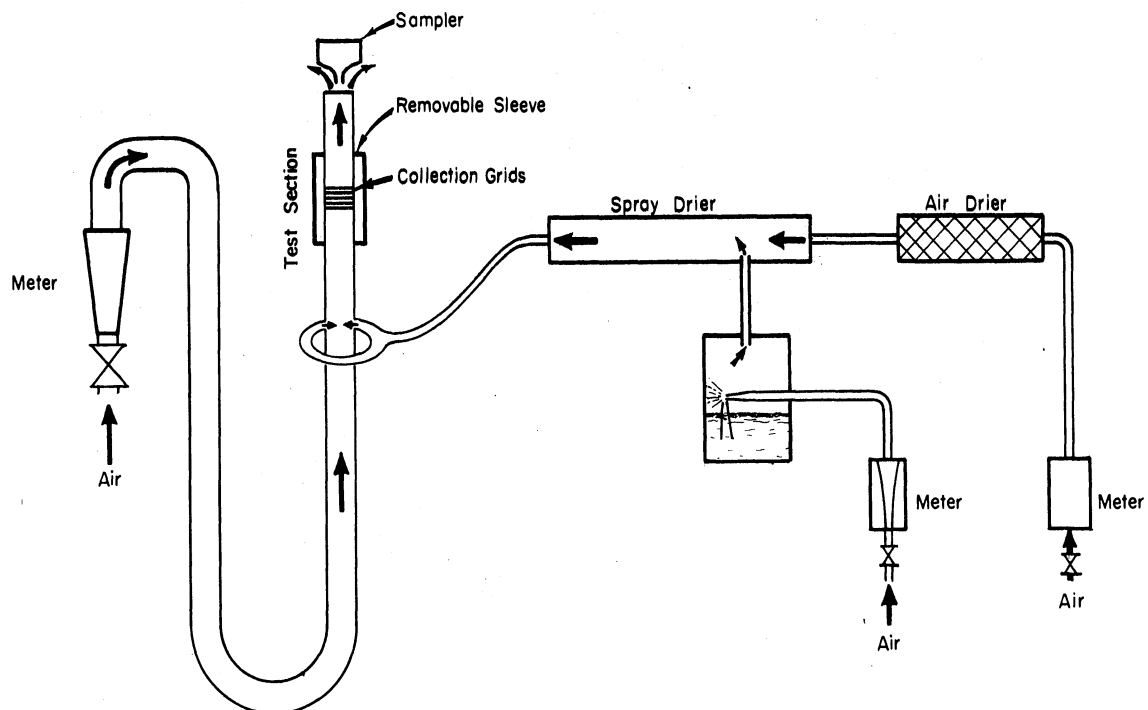
Meter

Air

Meter

Meter

Air

Air

Fig. 1. Test equipment.

1. The test section was made of 2-inch (ID) lucite tubing. It was built so that a number of brass rings, which supported the wires, could be stacked on top of a tube and another length of tubing placed on top of the stack. The assembly was held in place by a lucite sleeve and the result was a continuous duct of 2-inch internal diameter. The test grids were 27-3/4 inches above the salt-dust entrance. The removable sleeve permitted removal of the stack of test grids after a run so that the salt could be washed off in a beaker of water.

2. The test grids were brass rings to which 0.003-inch-diameter Alumel wire was glued in parallel lines 1/8 inch apart (center to center). The rings were 2 inches (ID) x 2-1/4 inches (OD) x 1/32 inch thick. In some runs blank rings were used as spacers. Some tests were also performed using circular pieces of 14-mesh copper wire screen (0.011-inch wire diameter) rather than the parallel grids.

3. The exit-air sampler was an isokinetic type, employing MSA 1106B glass-

fiber paper as the filtering medium. The ratio of total air rate to sampler air rate was 28.4. Isokinetic conditions were maintained by matching the sampler air rate to the mainstream air rate by a throttle valve and rotameter leading to an aspirator.

4. The salt-dust generation system involved an aspirating atomizer installed in a chamber containing a large volume of saturated salt (NaCl) solution. The spray was directed at one wall of the chamber so that large drops struck the wall and ran back down. The smaller drops were carried into the spray-drying chamber by the atomizing air. In the spray-drying chamber the drops were mixed with air which had been dried in a desiccant-packed tube. The dried salt particles were then transported through a 1/2-inch (ID) plastic tube to the test-section entrance. The entrance consisted of a "Y" tube connected to two 1/2-inch tubes entering the test section from opposite sides. Thus the salt-dust stream split into two portions which entered the test section through two diametrically opposed tubes.

5. The main air stream was supplied by an air-jet ejector pump and metered with a calibrated rotameter.

PROCEDURE

Collection efficiency was determined in this apparatus for groups of 12 and 24 parallel wire grids and for groups of 10 and 20 screen discs with several variations in spacing between grids. The amount of salt dust collected on the wires was determined by washing the wires in a known volume of distilled water and then analyzing for salt content by an electrical conductivity measurement. The concentration of salt dust in the air leaving the test section was determined by similar analysis of the salt retained on the filter paper in the isokinetic sampler. From these measurements one can compute the total dust load in the air approaching the collection wires and also the percent collected.

The isokinetic sampler was checked against an absolute filter and the agreement was considered adequate although not perfect. The major difficulty in making this comparison was that the rate of salt-dust generation was not uniform but varied from about 0.0045 gm/min to 0.0075 gm/min. The agreement between the sampler and the absolute filter was about ± 10%. Measurements of dust distribution around the test section were made, but since these could not be made simultaneously the results, which show as much as twofold variation, are not conclusive.

Dust-particle size was determined by a visual count of a sample collected on a microscope slide. The sample was collected by introducing the airstream from the dust-generator outlet tube into the top of a 1-foot-high, 3-inch-diameter tube which was set vertically over the slide and allowing the dust to settle on the slide. Several checks indicated consistency in this

method and there does not seem to be any sampling bias. The size distribution was quite constant and is shown on a logarithmic probability plot in Fig. 2.
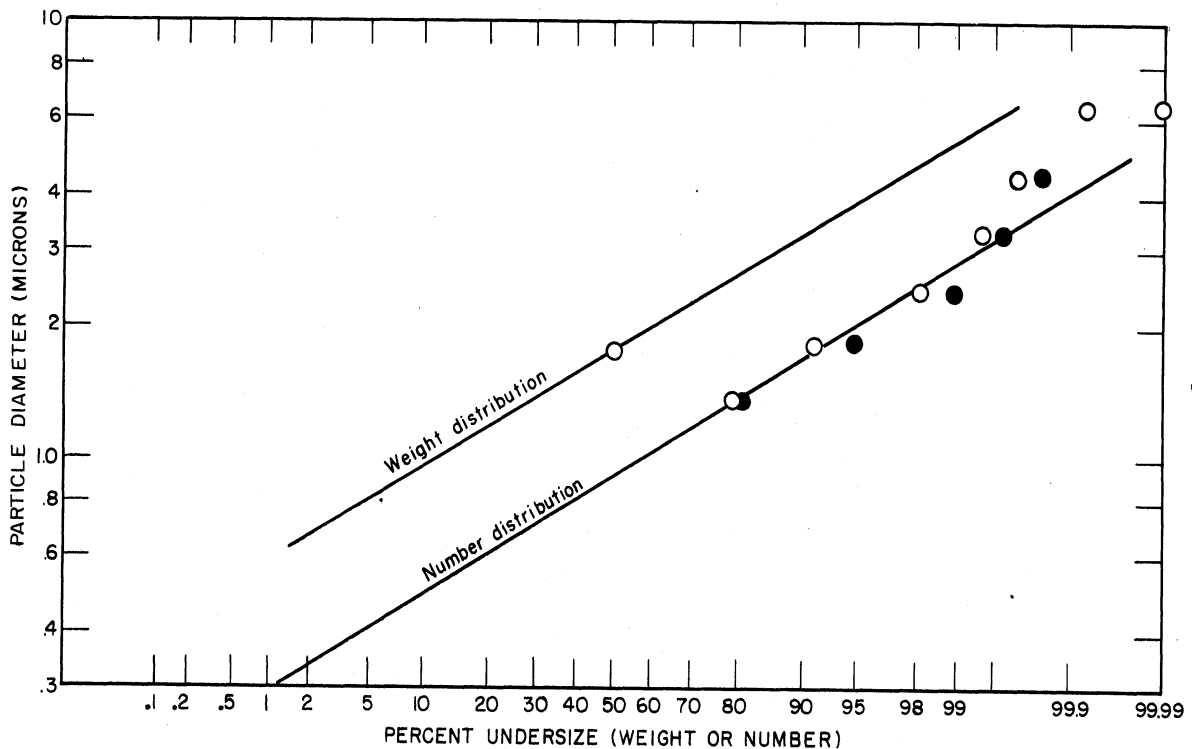

Fig. 2. Salt-dust size distribution.

Weight distribution was computed from number distribution by means of the formula

$$\ln X_g' \;=\; \ln X_g + 3(\ln \sigma_g)^2 \qquad ,$$

where

X_g = geometric mean diameter by number,

X_g' = geometric mean diameter by weight, and

σ_g = standard deviation.

RESULTS

      The experimental collection-efficiency data are shown in Figs. 3 and 4, which are plots of collection efficiency vs air velocity for the parallel wire grids and the wire screen, respectively. Also plotted on these figures are the dashed lines representing predicted collection efficiency, using the Langmuir and Blodgett data and assuming either complete mixing of the airstream or no mixing, as indicated on the plots. This prediction involves the use of collection efficiencies for single wires which are pre-

Fig. 4. Salt-dust collection efficiency vs air velocity (.011-in.-dia wire screen, .075-in. space, 14 mesh, 2-in.-ID tube, 1/32-in. vertical spacers).
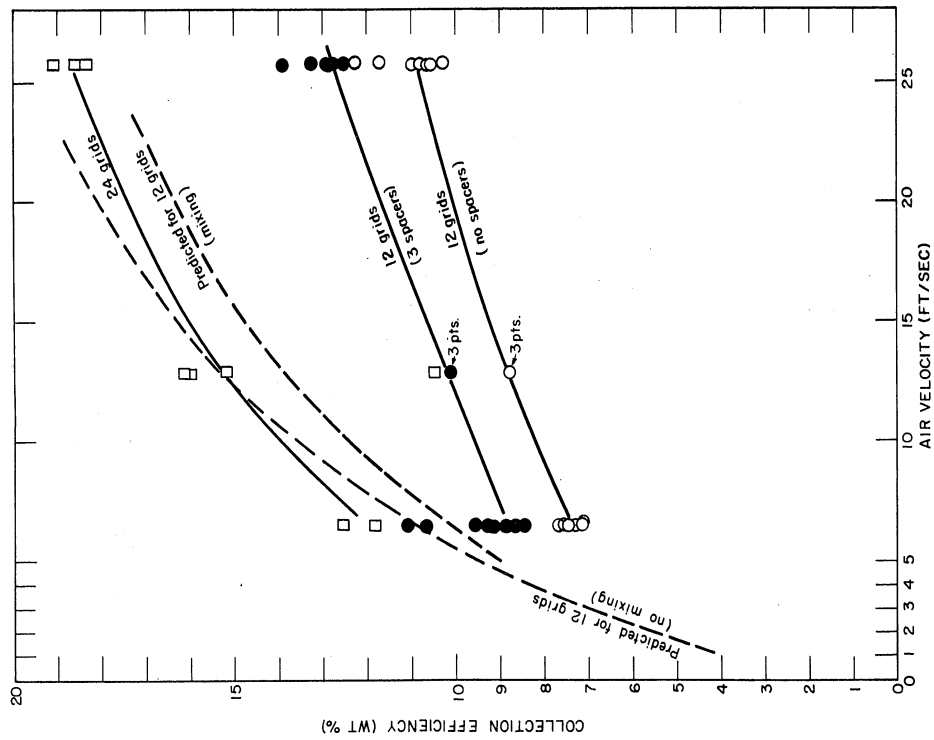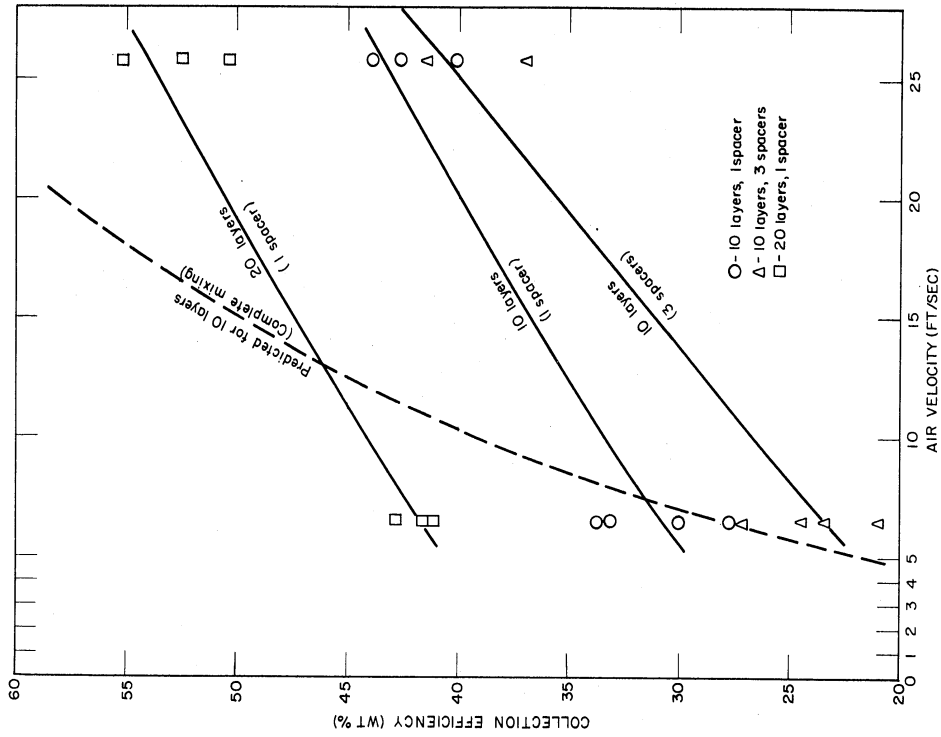
Fig. 3. Salt-dust collection efficiency vs air velocity (.003-in.-dia wire, 1/8-in. wire spacing, 2-in.-ID tube, 12 and 24 grids, 1/32-in. vertical spacers).

sented in Fig. 5, a plot of collection efficiency versus air rate with particle diameter as the parameter.
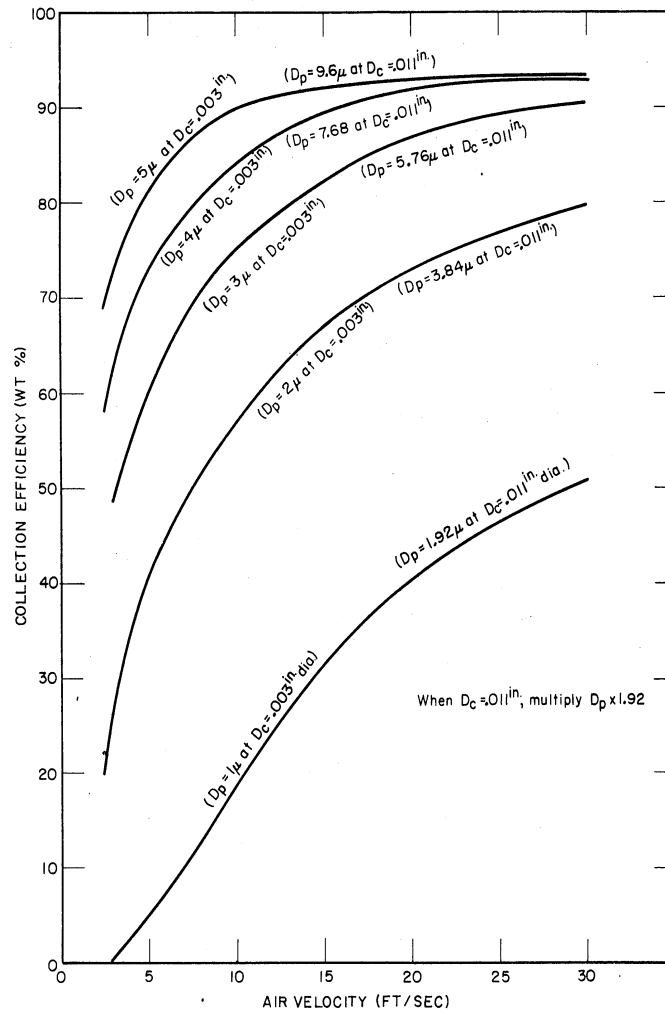

Fig. 5. Collection efficiency vs air velocity with particle diameter as parameter (NaCl on 0.003-in.-dia wire and 0.011-in.-dia wire).

DISCUSSION OF RESULTS

The most significant observation is that the predictions are close at low velocity but depart appreciably from the experimental data as velocity increases. The effect of increasing bed depth is in general agreement with the theory, although it is not possible to determine the amount of mixing from these data. There is a definite effect of axial spacing; but, since it is in opposite directions for the parallel wires and for the screens, any discussion of the mechanism involved would be purely speculative at this point.

The data obtained are not sufficient to establish any correlation, but they definitely indicate that collection efficiency is lower than pre-

dicted on the basis of the impaction mechanism. The obvious explanation is that some of the particles bounce off the collecting wires. An attempt was made to obtain some information on this by taking high-speed motion pictures and high-speed flash pictures of a dust-laden jet striking a wire. Unfortunately, there was not sufficient resolution in these pictures to show the particle trajectories.

A few exploratory runs were made using wires coated with Canada balsam to see whether this would raise collection efficiency, but it did not. The use of oil fog was also explored but the analytical difficulties made this brief study inconclusive, except for one point: that collection efficiencies for round jets striking flat plates were lower than predicted. Stated another way, this meant that the particle size passing through the impaction zone was larger than predicted.

The conclusion is that particulate collection efficiency is by no means completely described by the theoretically derived impaction efficiencies. The fact that predictions agree well with data for wetted wires can be considered fortuitous and may result from a different mechanism than has been assumed.